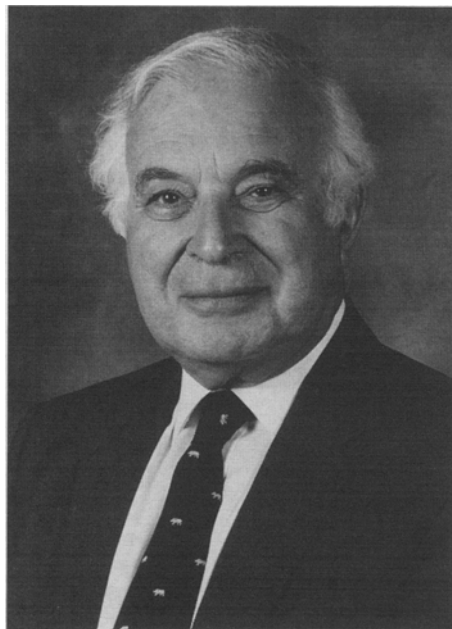


## Rafting in Superalloys

FRANK R.N. NABARRO



The phenomenon of rafting in superalloys is described, with particular reference to modern superalloys with a high volume fraction of the particulate  $\gamma'$  phase. It is shown that in the elastic regime, the thermodynamic driving force for rafting is proportional to the applied stress, to the difference between the lattice parameters of the  $\gamma$  matrix and the  $\gamma'$  particles, and to the difference of their elastic constants. A qualitative argument gives the sign of this driving force, which agrees with that determined by Pineau for a single isolated particle. Drawing on the work of Pollock and Argon and of Socrate and Parks, it is shown that after a plastic strain of the sample of order  $2 \times 10^{-4}$ , the driving force is proportional to the product of the applied stress and the lattice misfit, in agreement with the results of the calculations of Socrate and Parks. The rate of rafting is controlled by the diffusion of alloying elements. Here, the tendency of large atoms to move from regions of high hydrostatic pressure to those of low may outweigh the influence of concentration gradients. The deformation of the sample directly produced by rafting is small, of order  $4.5 \times 10^{-4}$ . The rafted structure is resistant to creep under low stresses at high temperatures. Under most experimental conditions at relatively high stresses, rafting accelerates creep; this effect may be less pronounced at the small strains acceptable under operational conditions.

---

FRANK R.N. NABARRO is Professor Emeritus at the University of Witwatersrand and in the Division of Materials Science and Technology, South African Council for Scientific and Industrial Research.

He received his early degrees from Oxford and his D.Sc. degree in metallurgy from Birmingham University. In 1949, he joined A.H. Cottrell in Birmingham and then worked with S.C. Hunter. He moved to the University of Witwatersrand in 1953. His research has concentrated mainly on dislocations, both within materials science and in other fields.

He has published the *Theory of Crystal Dislocations* and has edited nine volumes of *Dislocations in Solids*. He is a fellow of the Royal Society of London and past president of the Royal Society of South Africa and has three honorary degrees.

*The Institute of Metals Lecture was established in 1921, at which time the Institute of Metals Division was the only professional division within the American Institute of Mining and Metallurgical Engineers. It has been given annually since 1922 by distinguished people from this country and abroad. Beginning in 1973 and thereafter, the person selected to deliver the lecture will be known as the "Institute of Metals Division Lecturer and R.F. Mehl Medalist" for that year.*

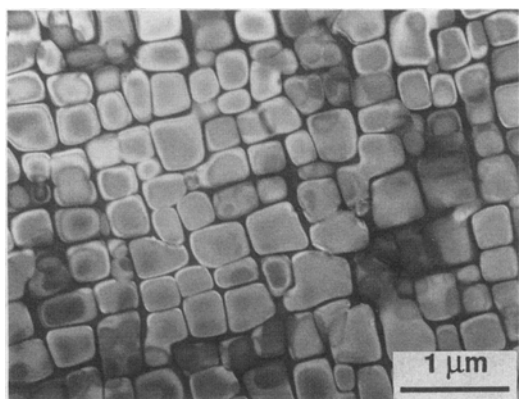
### I. INTRODUCTION

A typical modern superalloy for first stage turbine blades is a single crystal containing almost cubical particles of an ordered phase stacked in a very close approximation to simple cubic packing in a disordered alloy matrix (Figure 1). The ordered phase is called  $\gamma'$  and is based on the L1<sub>2</sub> structure of Ni<sub>3</sub> Al (Figure 2). The disordered matrix is a ductile close-packed cubic Al lattice. The difference between the lattice parameters  $a_{\gamma'}$  and  $a_{\gamma}$  of the two cubic structures is measured by the lattice misfit  $\delta$ , defined by

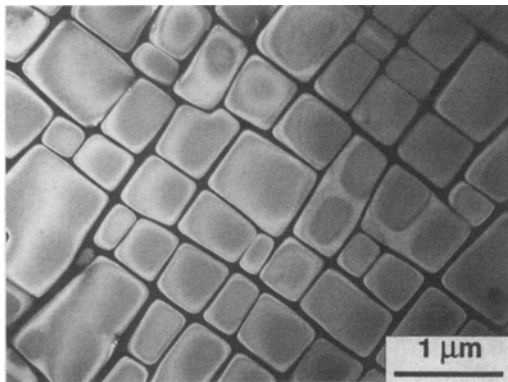
$$\delta = \frac{2(a_{\gamma'} - a_{\gamma})}{a_{\gamma'} + a_{\gamma}} \quad [1]$$

We also define the fractional difference in elastic moduli  $M$ :

$$m = \frac{2(M_{\gamma'} - M_{\gamma})}{M_{\gamma'} + M_{\gamma}} \quad [2]$$



(a)



(b)

Fig. 1—Transmission electron microscope superlattice dark-field images of  $\gamma'$  precipitates in MXON: (a) before and (b) after heat treatment.<sup>[1]</sup>

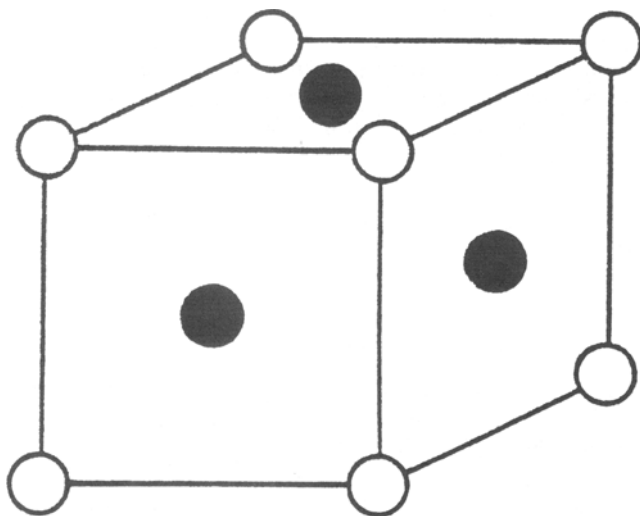


Fig. 2—Unit cell of  $\text{Ni}_3\text{Al}$ ; Ni atoms are on face centers and Al atoms are at corners.

It turns out that the relevant modulus is

$$M = c_{11} - c_{12} \quad [3]$$

For current commercial superalloys,  $\delta$  is usually negative and very small. One of our tasks will be to explain both the sign and the very small magnitude of this quantity.

There are few if any direct measurements of  $m$  at operating temperatures. Estimates involving extrapolation and

argument from analogy usually lead to positive values of  $m$  of order 0.1.

This single crystal forms a turbine blade which is stressed at high temperatures, predominantly by centrifugal force in tension along a cube axis. Under the combined influence of stress and temperature, the cubic particles transform into flat shapes which are usually called rafts (Figure 3(d)). If the tensile stress is replaced by a compressive stress along the same axis, needles (Figure 3(c)) or platelets (Figure 4) are formed parallel to the stress axis.

There are other alloys in which this behavior is reversed, with needles parallel to the axis of stress being formed in tension and rafts perpendicular to the axis in compression (Figures 5(b) and (c)).

We need to understand both the driving force for these transformations and the factors which control the rate of transformation. The driving force may alter substantially if plastic flow occurs in the ductile  $\gamma$  matrix.

Since the transformations are induced by the applied stress, the stress must do work while the shape changes are taking place, and this means that the sample as a whole must be slowly yielding to the applied stress, that is to say, creeping. Finally, when the shape transformation is nearing completion, we are left with a material whose microstructure is very different from that of the original material, and other mechanisms of creep will occur faster or slower than they would in the original microstructure.

## II. SOME GEOMETRICAL CONSIDERATIONS

Why does this tidy cubical array form in the first place? Essentially, this morphology depends on the elastic anisotropy of the  $\gamma$  matrix. Think first of an isolated spherical particle inserted in a spherical cavity which is slightly too small for it. In isotropic elasticity, the strains are purely dilatational in the particle and purely shear in the matrix (Figure 6).

Suppose this statement remains roughly true for a cubical particle when the elastic contents have cubic symmetry. In cubic symmetry, there are two shear constants  $c_{44}$  and  $\frac{1}{2}(c_{11} - c_{12})$ , corresponding to the distortions sketched in Figure 7. For the materials with which we are concerned, the deformation with modulus  $c_{44}$  is harder than that with modulus  $\frac{1}{2}(c_{11} - c_{12})$  by a factor of about 3.4. If the strain inside the particle remains dilatational, its internal elastic energy is independent of its shape. If the particle adopts the shape of a cube aligned with the crystal axes, most of the matrix outside it is strained in the easy shear mode, and the energy is minimized. This concentration of the shear strain in the matrix into easy directions is even stronger when the cubes are packed together. These rough arguments are confirmed by the more realistic computer calculations of Pollock and Argon<sup>[5]</sup> (Figure 8).

In most of the  $\gamma'$  matrix, the negative hydrostatic pressure of about 80 MPa exceeds the von Mises shear stress of about 60 MPa, while in most of the  $\gamma$  matrix, the hydrostatic pressure of about 250 MPa is less than the von Mises shear stress of about 430 MPa.

For the particles with which we are concerned, the influence of elastic energy greatly outweighs that of surface energy. Surface energy tends to produce roughly spherical particles and dominates only for particles with radii smaller

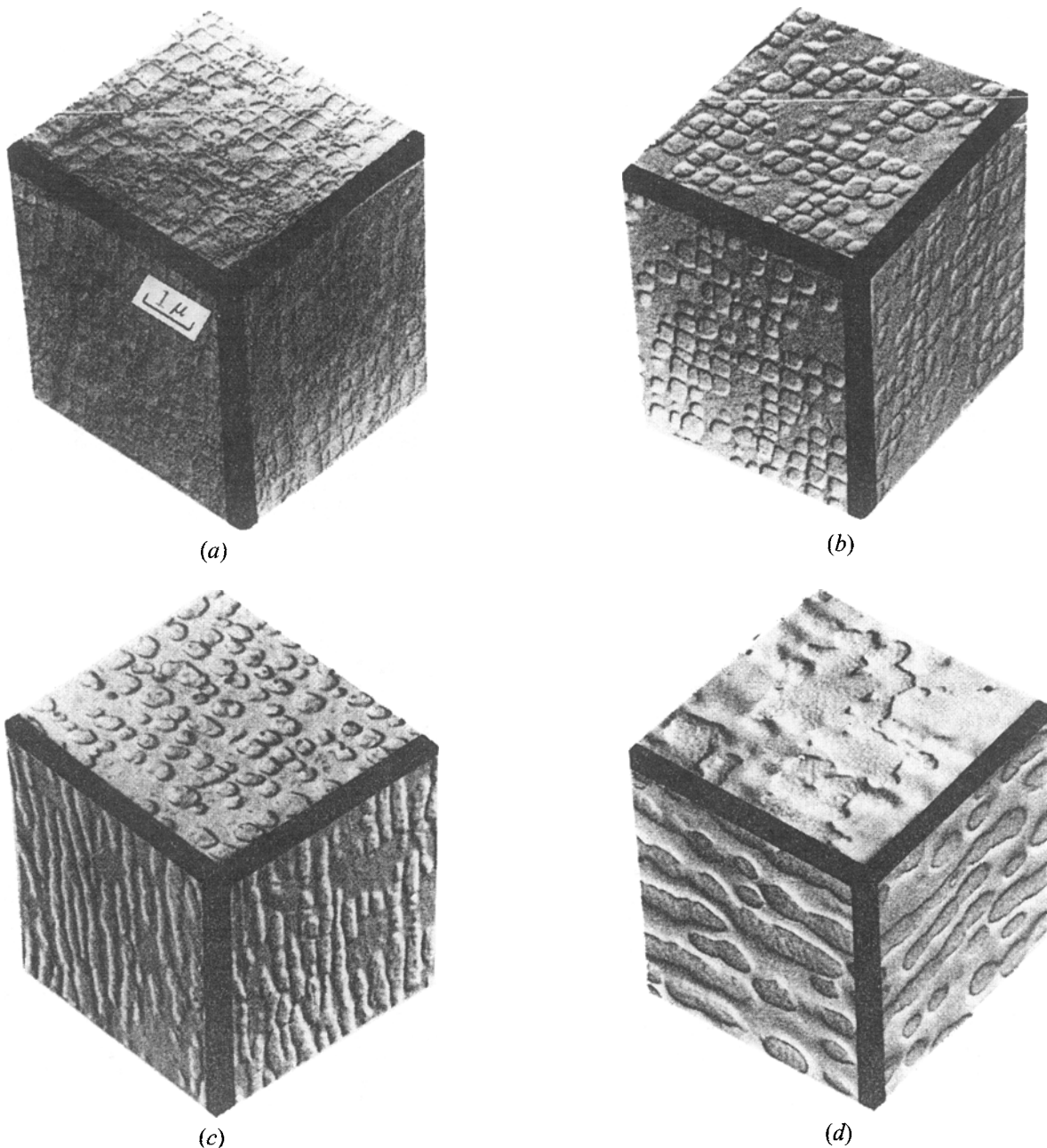


Fig. 3—Mounted replicas of cube faces of superalloy: (a) after standard heat treatment and after additional annealing for 100 h at 954 °C, (b) without applied stress, (c) under compressive stress normal to the top face, and (d) under an equal tensile stress.<sup>[2]</sup>

than the radii of curvature of the edges of the slightly rounded cubes which are actually formed. Since surface energy is negligible, the theory of phase equilibria tells us that the total volume of the  $\gamma'$  particles remains constant as their shape changes. As can be seen from Figure 9, this prediction is verified for samples annealed with or without stress for times so long that those with stress first form rafts and then form more equiaxed semicoherent shapes. Ideally, the number of particles remains constant during the early stages of rafting, which would lead to a shrinking of the  $\gamma'$  particles along the tensile axis as their transverse dimensions increase, while the layers of  $\gamma$  matrix normal to the tensile axis thicken. This early stage of rafting is shown in Figure 10.

Then adjacent particles meet and fuse together producing extended rafts (Figure 11). The thickness of the  $\gamma'$  particles

has not changed greatly, as may be seen by comparing the main portion of Figure 11 with the insert, which is part of Figure 10 reduced to the same scale as the rest of Figure 11.

In fact, the total number of particles decreases during the early stages of rafting by the usual process of Ostwald ripening, and this coarsening then continues slowly. As a result, the thickness of the  $\gamma'$  particles normal to the tensile axis first decreases slightly and then increases, while the layers of  $\gamma$  parallel to the particles thicken rapidly at first and then slowly (Figure 12).

Rafting also occurs when an alloy with a matrix of B2 structure based on NiAl containing precipitates of an L2<sub>1</sub> Heusler alloy based on Ni<sub>2</sub>AlTi is annealed under stress.<sup>[9]</sup> In this case, there is a large positive misfit of order several percent, the precipitates are semicoherent, and platelets are formed parallel to an [001] tensile axis.

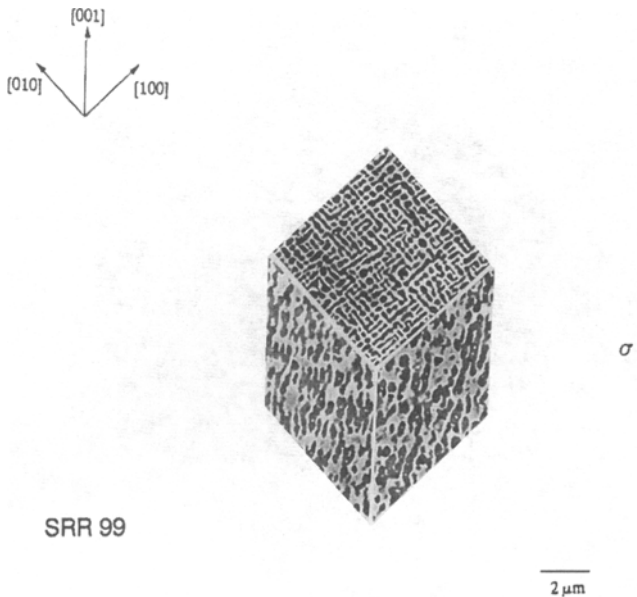


Fig. 4—Formation of platelets parallel to the compressive axis in SRR99.<sup>[3]</sup>

What happens if we anneal the regular cubic structure for a long time without an applied stress? At first, the  $\gamma$  and  $\gamma'$  lattices will remain coherent, and the behavior is governed by a theorem due to Khachaturyan;<sup>[10]</sup> the minimum strain energy at a given inclusion volume is attained if the inclusion is “rolled out” to give an infinite platelet of infinitesimal thickness. Khachaturyan then goes on to determine the habit planes, which in our case are clearly the cube planes. In our case, there are three equivalent sets of cube planes, so there is no clear pointer to the direction in which the process of rolling out should begin. In fact, the structure has some degree of stability. If it is irregular, it becomes regular on annealing. If the pattern is already regular, it may simply enlarge its scale by Ostwald ripening (Figure 13).

Alternatively, clusters of  $\gamma'$  rafts parallel to the cube axes may form (Figure 5(a)), in general agreement with Khachaturyan's prediction for an isolated particle.

### III. DRIVING FORCE FOR RAFTING WHEN PLASTIC FLOW CAN BE NEGLECTED

Suppose, for a given material, that a tensile stress along a cube axis causes the  $\gamma'$  cubes to extend transversely to the stress axis. Then experiments show that a compressive stress causes a longitudinal extension. So the thermodynamic driving force for rafting is directly proportional to the applied stress.

Suppose the  $\gamma'$  and  $\gamma$  phases had the same lattice parameters, *i.e.*, the misfit was zero. Then the process of rafting would simply replace some atoms by other atoms occupying exactly the same positions, and the external shape of the sample could not be altered. If the external shape of the sample is not altered, the applied stress does no work, and

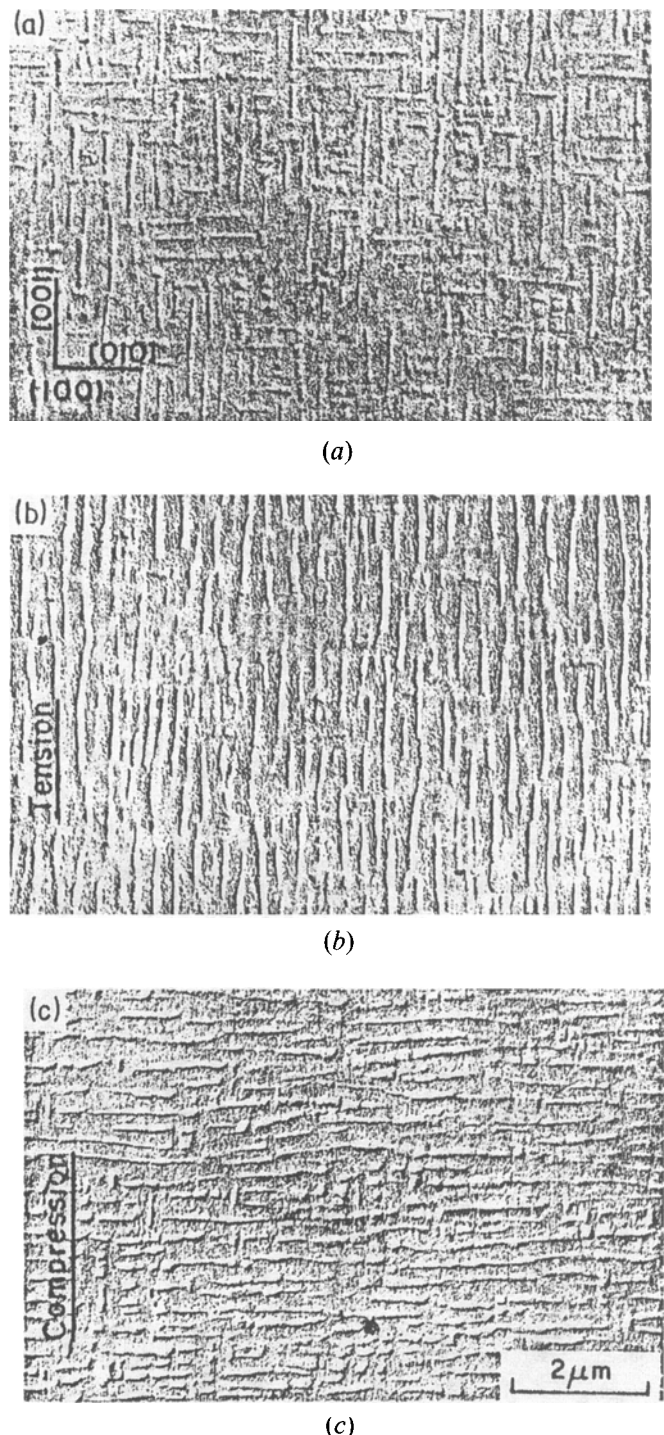


Fig. 5—Lateral face of an alloy with a large positive misfit of 0.56 pct annealed for 160 h at 750 °C: (a) without applied stress, (b) with tensile stress of 147 MPa, and (c) with equal compressive stress.<sup>[4]</sup>

so it cannot drive the process of rafting. The thermodynamic driving force for rafting must therefore be proportional to the misfit. In practice, alloys with a negative misfit at the working temperature, and these are usually the alloys of practical importance, tend to form rafts perpendicular to a tensile stress, while those with a positive misfit tend to form particles elongated parallel to a tensile stress. So the thermodynamic driving force is proportional to the product of the applied stress and the misfit.

What about the difference in the elastic moduli of the

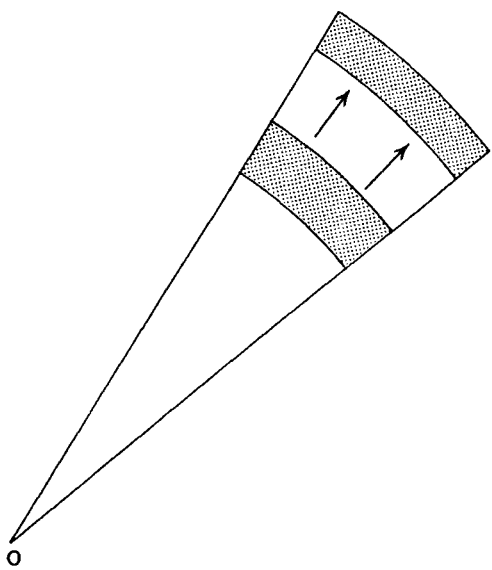


Fig. 6—The material outside a dilated sphere is sheared without a change of volume.

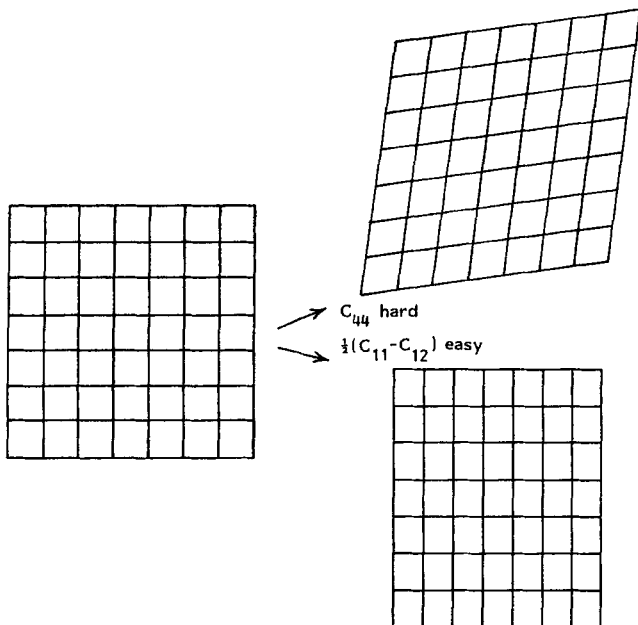


Fig. 7—Hard and easy shear distortions of the  $\gamma'$  phase.

two phases, which appears in Pineau's pioneering calculations<sup>[12]</sup> for the rafting of an isolated particle? We can show that the thermodynamic driving force for rafting must also be proportional to this difference, as long as no plastic flow occurs. To see this, consider a single  $\gamma'$  particle embedded in a matrix of  $\gamma$ , and, to fix our ideas, suppose that the misfit is negative. There is no external stress (Figure 14(a)). Suppose that  $\gamma'$  and  $\gamma$  have the same elastic constants. Suppose also that the work which has to be done to assemble the misfitting components in proper atomic register in the absence of an applied external stress is  $W_a$ . Now we disassemble the composite body (Figure 14(b)), and we recover the work  $W_a$ , so the work we do in this process is  $-W_a$ . Now apply a uniform tensile stress  $\sigma$  to both components (Figure 14(c)). If the volumes of the two components in the absence of stress are  $V_{\gamma'}$  and  $V_{\gamma}$ , and their Young's moduli are  $E$ , the work done is  $1/2(V_{\gamma'} + V_{\gamma})\sigma^2/E$ .

Because we have assumed that  $\gamma'$  and  $\gamma$  have the same elastic constants, the  $\gamma'$  component and the hole in the  $\gamma$  matrix have changed their shapes by exactly the same amount, and the forces acting on matching positions of their surfaces are equal and opposite. Now reassemble the structure under stress (Figure 14(d)). Apart from trivially small terms, the work required is simply  $W_a$ , and we have an elastically homogeneous body in equilibrium under a uniform tensile stress. If we release the stress, we do an amount of work  $W$  and the system is back in its original state (Figure 14(a)). Since the total work done in the cycle must be zero, it follows that

$$-W_a + \frac{1}{2}(V_{\gamma'} + V_{\gamma})\sigma^2/E + W_a + W = 0 \quad [4]$$

or

$$W = -\frac{1}{2}(V_{\gamma'} + V_{\gamma})\sigma^2/E \quad [5]$$

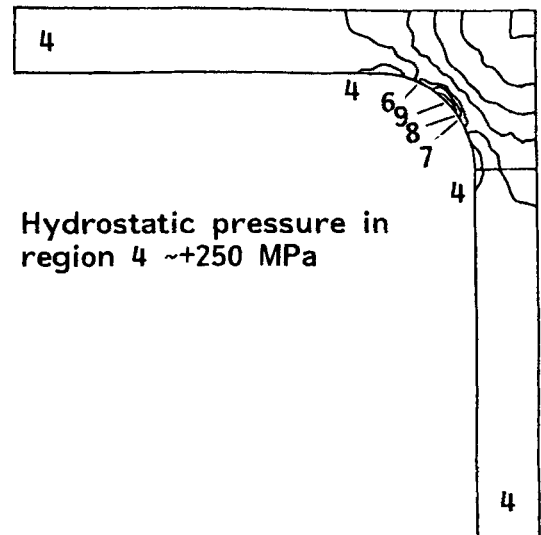
If, instead of releasing the stress, we had applied the stress  $\sigma$  to the compound body, we would have done work

$$-W = \frac{1}{2}(V_{\gamma'} + V_{\gamma})\sigma^2/E \quad [6]$$

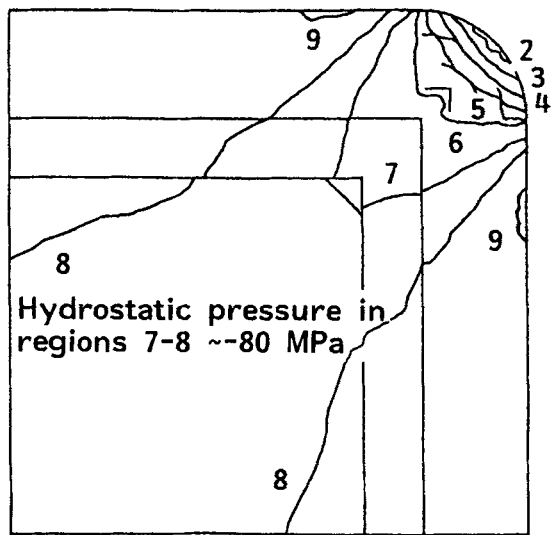
Provided that the  $\gamma'$  and  $\gamma$  components can be brought into atomic register, this work depends only on their volumes and not on the shape of their interface. The work done by an applied stress is the same regardless of whether the alloy has rafted. In other words, the applied stress does no work when rafting occurs, and an applied stress cannot drive the process of rafting if  $\gamma'$  and  $\gamma$  have the same elastic constants. The thermodynamic driving force must be proportional to the difference of the elastic constants. Thus, the thermodynamic driving force is proportional to the applied stress, which is a fraction of 1 percent of the modulus; to the misfit parameter, which is usually a fraction of 1 percent; and to the difference of the elastic constants, which is of order one-tenth of the constants themselves. It is a very small and subtle quantity.

Can we nevertheless predict the sign of rafting in a particular case? A simple argument is sometimes advanced. Suppose we consider the case in which  $\gamma'$  has a smaller lattice parameter than  $\gamma$ , and a smaller elastic constant, and a tensile stress is applied along a cube axis. In these simple arguments, we neglect the Poisson contraction, which is a plausible approximation. The sheets of  $\gamma$  are much thinner than the width of the  $\gamma'$  cubes, and so, when the two are brought into register, the  $\gamma$  sheets are compressed far more than the  $\gamma'$  cubes are stretched, and most of the elastic energy of misfit is stored in the  $\gamma$  sheets. Now suppose that instead of assembling a supercell consisting of a  $\gamma'$  cube and its six cladding sheets of  $\gamma$  (Figure 15) from unstressed components, we assemble them under a uniform tensile prestress. Because it is elastically softer, the  $\gamma'$  cube will have stretched more than the lateral  $\gamma$  sheets, the misfit will be reduced, and the work of assembly is less than it would have been in the absence of the external stress. This economy is effected in fitting the lateral plates and is greater when the area of the lateral plates is larger, that is to say, when the  $\gamma'$  cubes elongate into needles parallel to the tensile axis.

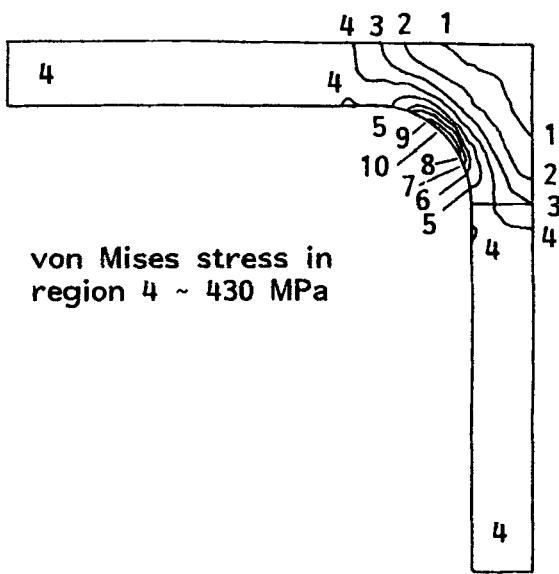
The answer is correct, but the argument is faulty in many ways. First, a transformation is favored by an external stress



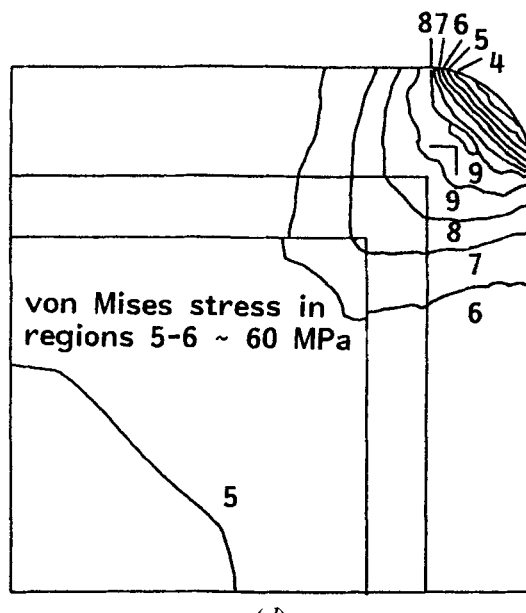
(a)



(b)



(c)



(d)

Fig. 8—Misfit stresses in CMSX-3 without external load: (a) and (b) hydrostatic pressure; and (c) and (d) von Mises shear stress, redrawn from Ref. 5 with the kind permission of Elsevier Science Ltd., Kidlington, United Kingdom.

when the work done by the stress during the transformation exceeds the increase in the internal energy produced by the presence of the stress during the transformation. The relevant chemical potential is the enthalpy, not the energy. The present argument completely neglects the work done by the external stress. Second, the argument purports to depend on the change of the internal energy produced by the presence of an external stress. An old theorem due to Colonnetti<sup>[13]</sup> shows that this change is precisely zero. We shall outline a valid qualitative argument which leads to the same result.<sup>[14]</sup> It depends on a special application of Eshelby's energy-momentum tensor<sup>[15,16]</sup> to this particular problem.

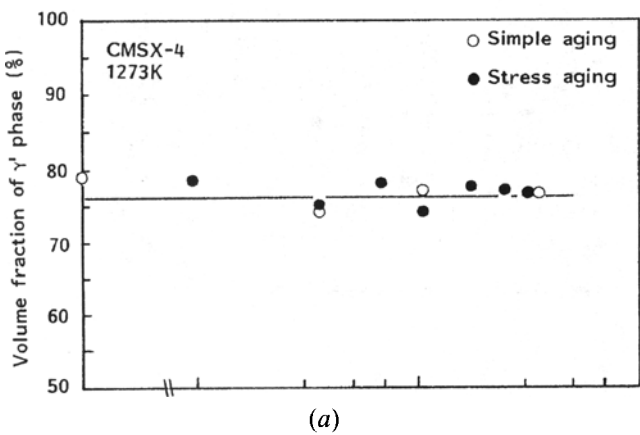
#### IV. THE RESULT OF A FORMAL CALCULATION IN THE ELASTIC REGIME

A formal calculation has been carried out,<sup>[14]</sup> using the formalism of Eshelby's energy-momentum tensor,<sup>[15,16]</sup> as

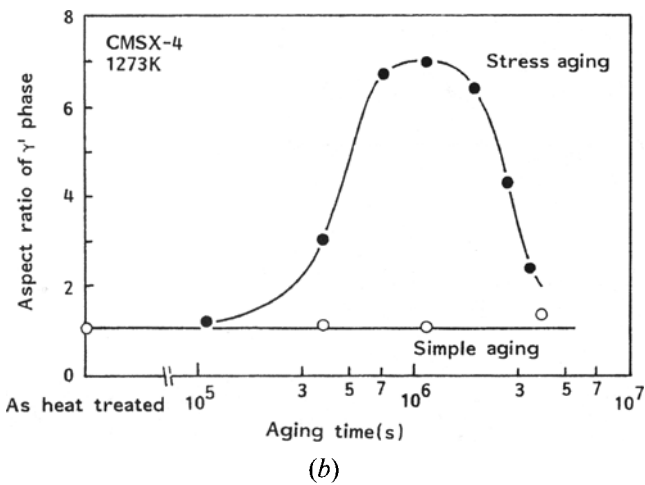
developed by Socrate and Parks<sup>[17]</sup> for this problem, subject to a number of assumptions:

- (1) the  $\gamma'$  particles are constrained to remain square-based prisms;
- (2) the distortion from a cubic shape is small;
- (3) the thickness of a  $\gamma$  sheet is always small in comparison with the side of a  $\gamma'$  cube (in practice, this ratio  $\tau$  is about 0.15);
- (4) the fractional differences  $m$  and  $n$  of elastic constants between  $\gamma'$  and  $\gamma$  are small (in practice, the fractional differences  $m$  and  $n$  are about 0.15 pct); and
- (5) squares and products of  $\tau$ ,  $m$ , and  $n$  may be neglected.

The result is that the energy dissipated when a cube of  $\gamma'$  of dimensions  $wa \times wa \times wa$  becomes a raft of dimensions  $(1 + \varepsilon)wa \times (1 + \varepsilon)wa \times (1 - 2\varepsilon)wa$  under the influence of a tensile stress  $\sigma$  is



(a)



(b)

Fig. 9—(a) Changes in the volume fraction of  $\gamma'$  during simple aging and aging under stress of CMSX-4; and (b) corresponding changes in the aspect ratio of  $\gamma'$  particles. Originally published in Ref. 6.

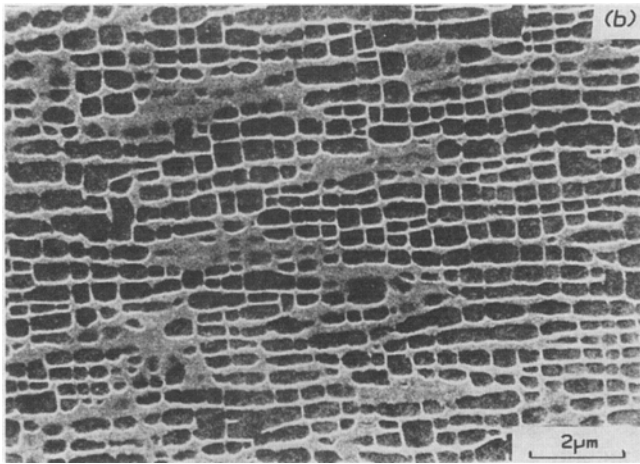


Fig. 10—An early stage of rafting.<sup>[7]</sup>

$$-2 w^3 a^3 \varepsilon \frac{[c'_{11} - c_{11}] - (c'_{12} - c_{12})}{c_{11} (c_{11} - c_{12})} (c_{11} + 2c_{12}) \delta o \quad [7]$$

Elastic stability requires that each of the factors  $c_{11}$ ,  $c_{11} + 2c_{12}$ , and  $(c_{11} - c_{12})$  is positive. In this approximation, there is no dependence on the fractional thickness  $\tau$  of the  $\gamma'$  sheets. The relative stiffness of  $\gamma'$  and  $\gamma$  is determined by the elastic constant  $c_{11} - c_{12}$ , and we may write

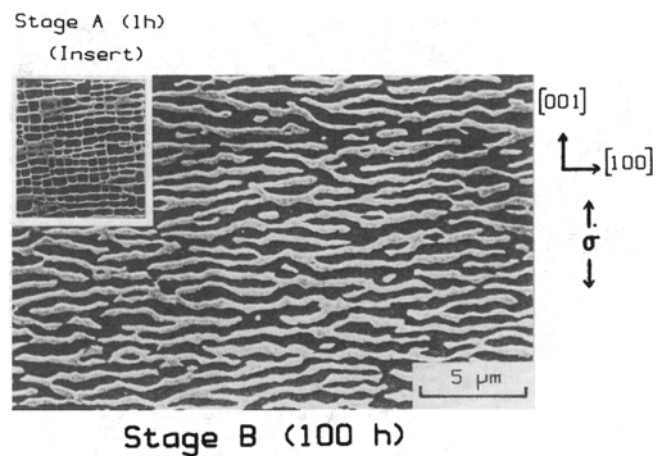


Fig. 11—A later stage of rafting. The thickness of the  $\gamma'$  particles has not changed greatly, as can be seen from the insert of Fig. 10 on the same scale.<sup>[7]</sup>

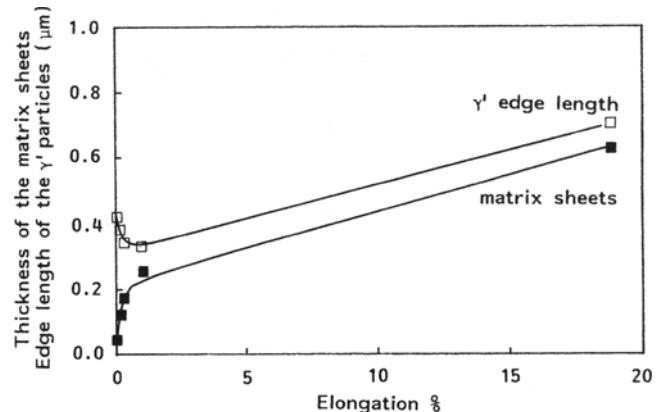


Fig. 12—Thickness of the  $\gamma'$  matrix sheets and edge length of the  $\gamma'$  particles during rafting of CMSX-4.<sup>[8]</sup>

$$c^* = (c'_{11} - c_{11}) - (c_{11} - c_{12}) \quad [8]$$

While the details of the calculation are very tedious, the underlying physics is clear. There are two components to the thermodynamic pressure tending to move an interface between two phases. One is clearly the difference in the energy densities on either side of the interface. Since we have chemical equilibrium, this energy density is simply the elastic energy density. We are dealing with a system under external stress, and so the behavior is governed by the enthalpy rather than the energy alone. We have to consider the work done by the external forces when the interface moves. Eshelby's calculations tell us that we do not need to work out the displacements of the surface of the body which occur when the interface moves. It is enough to calculate the work done in the neighborhood of the interface itself. In our case, the work done when the interface sweeps out unit volume is simply the product of the mechanical pressure  $p$  acting across the interface and the difference ( $e_n$ ) between the total strains normal to the interface on the two sides of this interface.

In the unstressed superalloy, the only large term is the energy density in the thin  $\gamma'$  sheets which are stretched or compressed to bring them into register with the cubes of

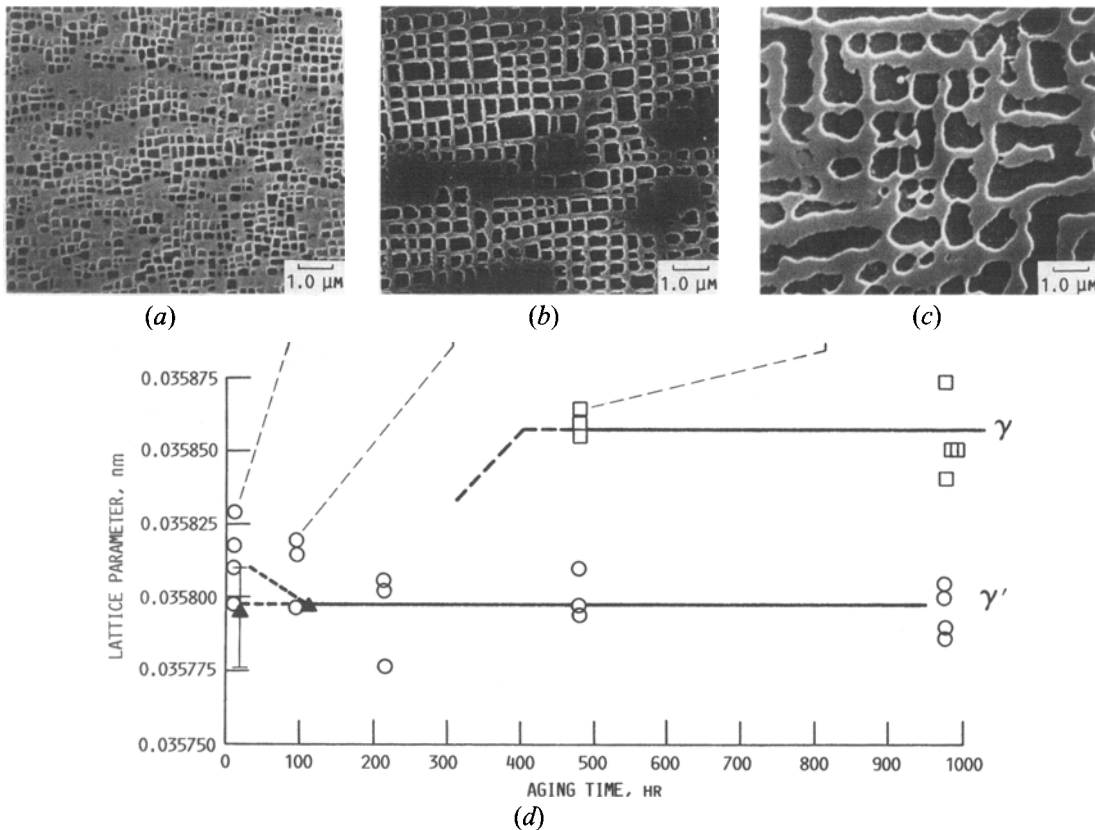


Fig. 13—In an experimental alloy similar to MAR-M200, the structure grows coherently with no separation of the  $\gamma$  and  $\gamma'$  diffraction peaks up to 200 h at 1000 °C (measured lattice parameters are ten times larger than those indicated). Reprinted from Ref. 11 with the kind permission of Elsevier Science Ltd.

$\gamma'$ . All the interfaces are subject to a thermodynamic pressure tending to move them outward and replace heavily strained  $\gamma$  by almost unstrained  $\gamma'$ . However, the volume fraction of  $\gamma'$  is constant, and this isotropic expansion of the  $\gamma'$  cubes cannot occur. The outward pressure produced by the elastic energy is balanced by an inward chemical pressure produced by a slight deviation of the compositions of  $\gamma$  and  $\gamma'$  from their equilibrium values in the unstressed state.

What happens if a small external stress  $\sigma$  is applied along a cube axis? This small stress will have little effect except in the regions where it interacts directly with a comparatively large pre-existing internal stress or strain. The lateral sheets of  $\gamma$  provide one of these regions. To fix ideas, suppose the  $\gamma'$  misfit is positive and the stress  $\sigma$  is tensile. Then  $\sigma$  increases the energy density in the lateral  $\gamma$  sheets by an amount of order  $\delta\sigma$ , which adds to the thermodynamic stress tending to move the lateral interfaces outward. On the transverse interfaces, the applied stress  $\sigma$  does work  $\delta\sigma$  per unit volume transformed if the interface moves outward, and this work adds to the thermodynamic pressure driving the transverse interfaces outward. It turns out that if  $\gamma'$  and  $\gamma$  have the same elastic modulus, the increases in thermodynamic pressure on the lateral and transverse interfaces are equal, and, because the volume of the  $\gamma'$  cube is fixed, they have no effect.

Now suppose that  $\gamma'$  is stiffer than  $\gamma$  by a fraction  $m$ . Then the lateral  $\gamma$  sheets will be restrained in their elongation under the tension  $\sigma$  by the underlying cubes of  $\gamma'$ .

The elongation will be reduced by a factor of  $1/(1 + m) \approx 1 - m$ , the energy density will be reduced by the same factor, and the outward pressure on the transverse interfaces will exceed that on the lateral interfaces by a quantity of order  $m\delta\sigma$ , leading to the formation of needles parallel to the stress axis. A reversal in the sign of  $m\delta\sigma$  reverses the type of rafting.

This is the rule established by Pineau<sup>[12]</sup> for an isolated particle in the absence of plastic flow.

## V. DISLOCATION MOTION IN THE EARLY STAGES OF CREEP

In a properly heat-treated superalloy, there are very few dislocations in the sheets of  $\gamma$  and virtually none in the cubes of  $\gamma'$ . Under stress along a cube axis, the dislocations in the  $\gamma$  sheets begin to move within these sheets and to multiply.

They move under the influence of stresses which are the result of the ingrown misfit stresses and the applied stress. These resultant stresses will obviously be different in the sheets of  $\gamma$  normal to the applied stress and in the sheets parallel to this stress. In the specific case of a tensile stress applied to an alloy with a negative misfit, dislocations move predominantly in the sheets normal to the stress axis (Figure 16). Reversal of the sign of  $\sigma$  or of  $\delta$  will cause the dislocation motion to alternate between normal and parallel  $\gamma$  sheets. Because the stress axis is an axis of fourfold sym-

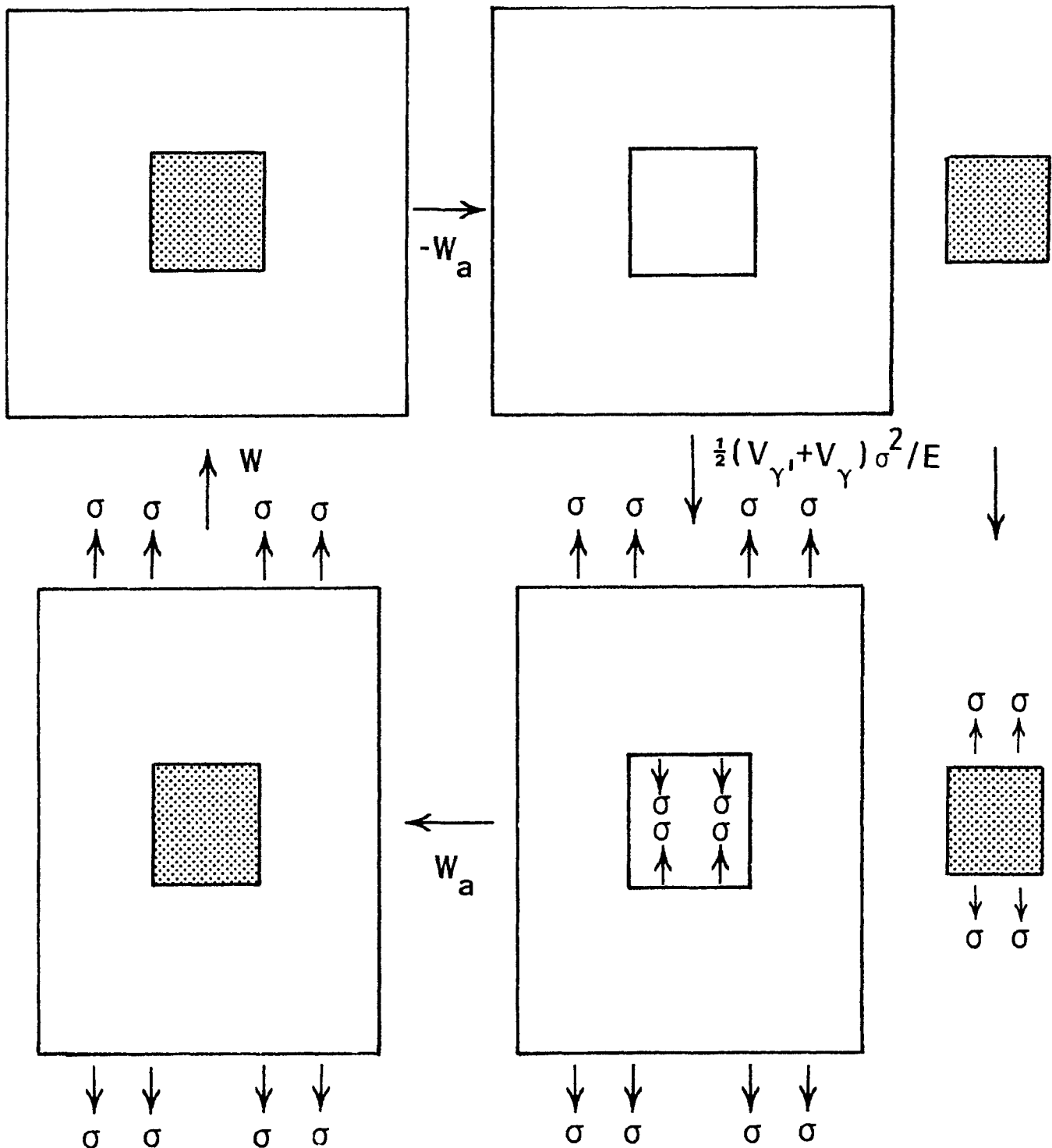


Fig. 14—(a) through (d) A homogeneously elastic inclusion is disassembled, loaded, reassembled under load, and then unloaded.

metry and the system is centrosymmetric, many glide systems of the face-centered cubic matrix are equally stressed.

These systems interact in a complicated way<sup>[18]</sup> to produce networks of dislocations on the  $\gamma/\gamma'$  interfaces which accommodate the misfit. For a stress along a cube axis, the force per unit length has a value which either is zero or has the same magnitude for all systems. Glide actually occurs on those systems for which the external stress and the misfit stress produce forces of the same sign, and therefore,<sup>[19]</sup> the

flow of dislocations is in general directed to relieving the misfit stresses. There is an argument<sup>[19]</sup> which extends this idea to account satisfactorily for the orientations of the rafts produced by tensile or compressive stresses along axes of low symmetry, claiming that as a result of the dislocation motion, "... a local gradient of coherency stresses will exist between the faces of the same precipitate. Under the influence of this gradient, the matrix atoms will diffuse from the faces where the misfit is not relaxed toward the

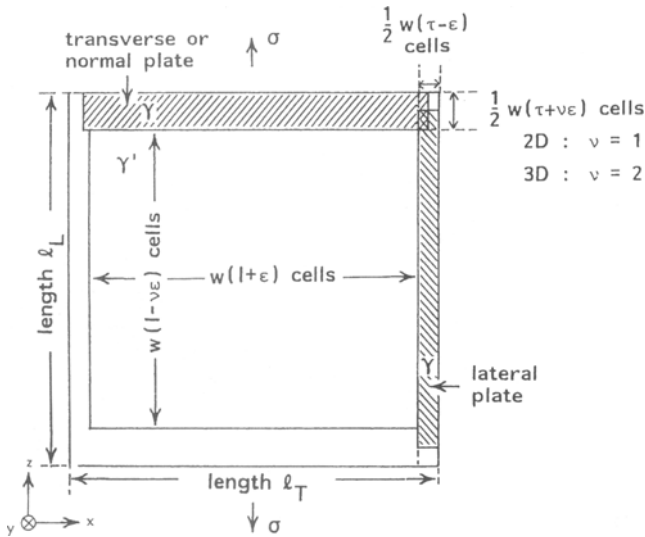


Fig. 15—The unit supercell in a superalloy, showing transverse (normal) and lateral  $\gamma$  sheets in lattice register with a  $\gamma'$  particle which has rafted to an extent  $\varepsilon$ .

faces where the misfit is relaxed.” The argument does not involve the difference  $c^*$  between the elastic constants of  $\gamma'$  and  $\gamma$  and, therefore, belongs to the discussion of rafting occurring after appreciable creep strain, presented in Section VI.

## VI. RAFTING AFTER APPRECIABLE CREEP

After the incubation period during which dislocations in the  $\gamma$  matrix are multiplying, the matrix contains dislocations moving on many slip systems and may be modeled as a non-Newtonian viscous fluid.<sup>[5,17,20]</sup> The elastic constant mismatch  $c^*$  between inclusion and matrix is no longer important. The mechanical properties of the plastic  $\gamma$  phase no longer approximate closely to those of the  $\gamma'$  phase, which is still elastic.

We can now extend the previous argument to see what happens when plastic flow begins in the  $\gamma$  matrix. Flow begins in those sheets in which the shear component of the applied stress adds to that produced by the coherency stresses. If  $\sigma\delta$  is positive, these will be the lateral sheets; in the more usual case of negative  $\sigma\delta$ , these will be the transverse sheets. These plastic flows will upset the delicate balance between the thermodynamic pressures tending to move the lateral and the transverse interfaces outward. With positive  $\sigma\delta$ , plastic flow  $\varepsilon_p$  in the lateral  $\gamma$  sheets reduces the energy density in the lateral sheets by an amount of order  $\varepsilon_p\sigma$ , thereby reducing the outward thermodynamic pressure on the lateral interfaces, while the thermodynamic pressure on the transverse interfaces is unaffected by the plastic flow over the lateral interfaces. So if  $\sigma\delta$  is positive, needles are formed parallel to the axis of stress. If  $\sigma\delta$  is negative, plastic flow begins outside the transverse interfaces. If these interfaces are displaced outward, the volume of the plastic region is reduced, and the work done by the external forces is reduced by an amount  $\varepsilon_p\sigma$  per unit volume swept out by these interfaces. The thermodynamic pressure on these interfaces is reduced, while that on the

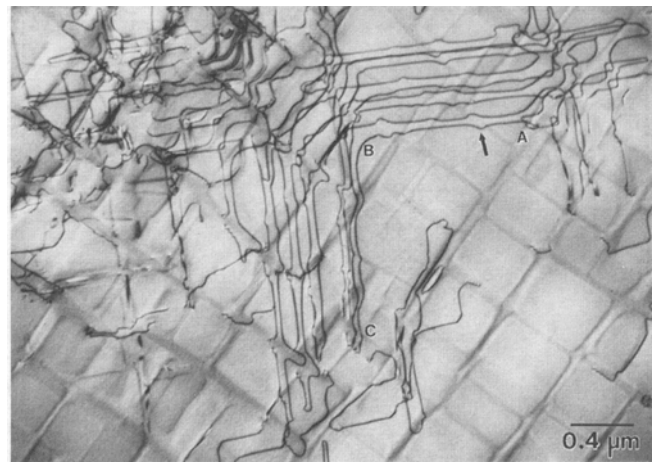


Fig. 16—Early stage of creep in CMSX-3. The dislocations move entirely in the  $\gamma$  matrix and almost entirely in the transverse  $\gamma$  plates. Reprinted from Ref. 5 with the kind permission of Elsevier Science Ltd.

transverse interfaces is unaltered. Rafts are formed normal to the stress axis.

These rules agree with those following from the calculations of Socrate and Parks.<sup>[17]</sup>

When the Pineau and the Socrate-Parks rules disagree, which will be the case when  $m$  is negative, the sense of rafting will reverse when the creep strain reaches a sufficient value.

The value, and even the sign, of  $m$  is rarely known, but it usually seems to be positive. According to the data of Yasuda *et al.*,<sup>[21]</sup> both Ni<sub>3</sub>Mn and Ni<sub>3</sub>Fe at room temperature have  $c_{11} - c_{12}$  higher in the ordered than in the disordered state. Typical values for Ni<sub>85</sub>Al<sub>15</sub> and some modern superalloys are shown in Table I. In all cases, except that of CMSX-3,  $m$  is positive. The negative value estimated by Pollock and Argon<sup>[20]</sup> for CMSX-3 depends on a number of assumptions and is incompatible with the observed direction of rafting at the low strains where the Pineau rules should be obeyed.

The transition from Pineau to Socrate-Parks rules should occur at very low strains. The thermodynamic pressure difference leading to rafting in the Pineau elastic regime is of order  $m\delta\sigma$ , while that in the plastic range is of order  $\varepsilon_p\sigma$ . If these are of opposite sign, the latter will overcome the former when  $\varepsilon_p \approx m\delta$ . With  $|m| \approx 0.1$  and  $|\delta| \approx 0.002$ , this gives  $\varepsilon_p \approx 0.0002$ . The transition has probably never been observed experimentally, but it appears very clearly in the calculations of Socrate and Parks for a hypothetical alloy with  $m = -0.1$  and  $\delta = +2 \times 10^{-4}$ . The predicted cross-over strain occurs when  $\varepsilon_p/\delta = |m| = -0.1$ . The observed crossover occurs between  $\varepsilon_p/\delta = (6 - 9) \times 10^{-5}$  and  $\varepsilon_p/\delta = (1.9 - 2.5)$  (Figure 17). In this figure, part (a) represents a quarter of the  $\gamma'/\gamma$  interface; “top” is transverse in our notation and “side” is lateral. Figure 17(b) shows a typical plot of the thermodynamic pressure tending to move the interface outward. In tension,  $m\delta\sigma$  is negative, and for small creep strains, we expect transverse rafting, represented by the inverse of Figure 17(b), as in Figures 17(c) and (d). Then when  $\varepsilon_p/\delta > |m|$ , the direction of rafting reverses (Figure 17(e)). In compression, these tendencies are reversed (Figures 17(f) through (h)).

Table I. Elastic Constants of  $\gamma'$  (Primed) and  $\gamma$  (Unprimed) for Four  $\gamma'/\gamma$  Alloys

Alloy	Reference	T (K)	$c_{11}'$ (GPa)	$c_{11}$	$c_{12}'$	$c_{12}$	$c_{11}' - c_{11}$	$c_{12}' - c_{12}$	$(c_{12}' - c_{12})$ to $(c_{11}' - c_{11})$
Ni <sub>85</sub> Al <sub>15</sub>	4	1023	166.6	112.4	106.5	62.7	54.2	43.8	10.4
CMSX-2	22	1050	124.8	109.3	67.1	58.7	20.5	8.4	12.1
SRR99	23	1253	205	187	133	129	18	4	14
CMSX-3	20	1100	182	206	126	142	-24	-16	-8

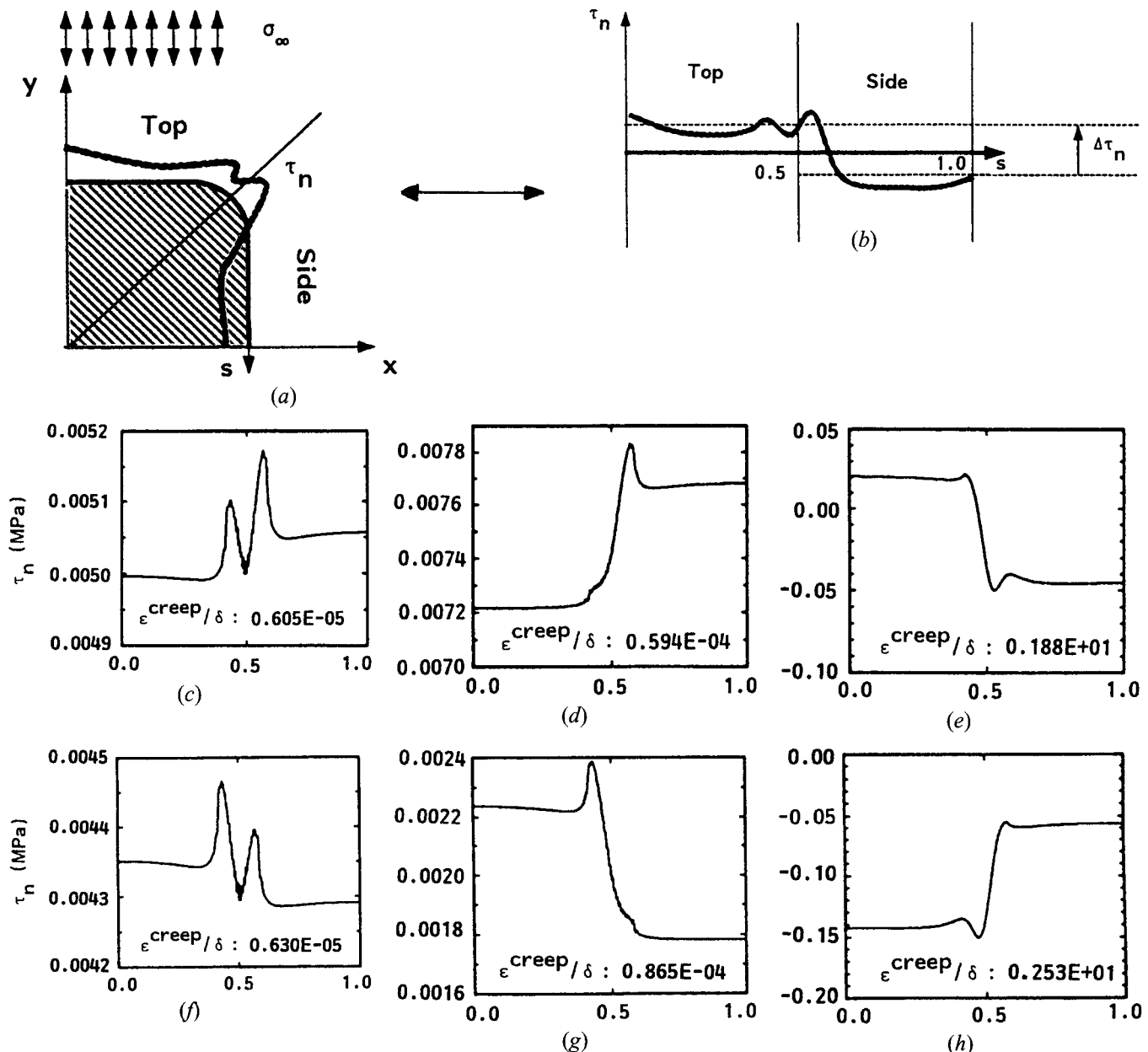


Fig. 17—(a) A quarter of a  $\gamma'$  cube, and the thermodynamic pressure tending to drive the  $\gamma'/\gamma$  interface outward; (b) the thermodynamic pressure as a function of distance along the interface, a case of parallel rafting; (c) through (h) Calculated curves for an alloy with  $\delta = +2 \times 10^{-4}$  and  $m = -0.1$ ; (c) through (e) under tension, for increasing strains; (f) through (h) under compression, for increasing strains. Reprinted from Ref. 17 with the kind permission of Elsevier Science Ltd.

The calculations of Socrate and Parks show that the thermodynamic driving force for rafting remains essentially constant as the plastic strain  $\epsilon_p$  in the  $\gamma$  matrix reaches val-

ues many times the misfit strain. The reason is probably that at least in their two-dimensional model, these large strains are numerically equal in the transverse and the lat-

eral channels, and the stresses they build up are numerically equal, and are simply superposed on the unsymmetrical stress distribution present at  $\varepsilon_p \approx |m\delta|$ .

## VII. COMPARISON WITH EXPERIMENT

In both the Pineau and the Socrate-Parks regimes, the sense of rafting reverses with reversal of the applied stress  $\sigma$ . This prediction is amply confirmed by experiments such as those illustrated in Figures 3 and 5. Several experimental observations of rafting appear to have been made in the Pineau regime. Thus,<sup>[7,24]</sup> an experimental alloy coded 221 with a misfit of  $\delta = -2.3 \times 10^{-3}$  showed substantial rafting after strains of  $\leq 2 \times 10^{-4}$ , and "lateral merging of adjacent  $\delta'$  cuboids . . . seems to precede dislocation multiplication." Pollock and Argon<sup>[20]</sup> studied an experimental alloy with a room-temperature misfit  $\delta = +7.7 \times 10^{-3}$ . Since<sup>[25,26]</sup>  $\delta$  usually decreases by at most  $4 \times 10^{-3}$  and usually  $1 \times 10^{-3}$  as the temperature increases from 0 °C to 800 °C to 1000 °C, their alloy probably had  $\delta > 3 \times 10^{-3}$  at their operating temperature of 1050 °C. It showed substantial rafting after a strain of only  $1.4 \times 10^{-3}$ .

However, because of the very small strain of order  $|m\delta|$  at which the transition to the Socrate-Parks regime is predicted to occur, most measurements have been made in this latter regime, where the behavior is controlled by the product  $\sigma\delta$ . The measurement of  $\delta$  is not easy; its sign may change between room temperature and the operating temperature,<sup>[2,4]</sup> and the data need to be considered critically. Socrate and Parks listed six experimental results which agree with their predictions and found no disagreements. In four of these six cases, their predictions were opposite to those of the Pineau regime.

## VIII. THE KINETICS OF RAFTING

Rafting is not an ordinary process of diffusional creep. The  $\gamma/\gamma'$  interface is coherent and does not provide a source or sink for vacancies. This is vividly illustrated by Figure 18, showing a simple nickel-based superalloy with 16 wt pct Cr, 5Al, and 4Ta after creeping under tension or under compression. The grain boundary zones depleted of or enriched in  $\gamma'$  particles confirm that the overall creep strain was of order 5 pct. In diffusional creep, the creep rate varies inversely as the square of the grain size. If the  $\gamma'$  particles, of diameter about  $0.4 \mu$ , crept by the same mechanism as the grains, of diameter diameter about  $60 \mu$ , their creep strain during the same test would be  $(60/0.4)^2 \times 5$  pct = 112,500 pct. If Coble creep was occurring, the strain would be even larger. In fact, the  $\gamma'$  particles are not visibly distorted, except for the particles touching a grain boundary, which have grown in size and distorted in the opposite sense to that of the sample as a whole.

If the superalloy consisted simply of cubes of ordered  $\text{Ni}_3\text{Al}$  in a matrix of disordered  $\text{Ni}_3\text{Al}$ , we could say that rafting occurred by diffusion of the order parameter along the interface from the transverse to the lateral boundaries. There would be no long-range transport of matter, as in diffusional creep, and no long-range diffusion of atoms from one face of the cube to another. All that is required is the interchange of neighboring or almost neighboring atoms. In practice,  $\gamma'$  and  $\gamma$  are alloys of different compo-

sitions, and the rate-controlling process is the diffusion of alloying elements, probably through the disordered  $\gamma$  phase, from one boundary to another. Those elements which are concentrated in the  $\gamma'$  phase should show a high concentration in the  $\gamma$  channels which are widening and a low concentration in those which are narrowing.

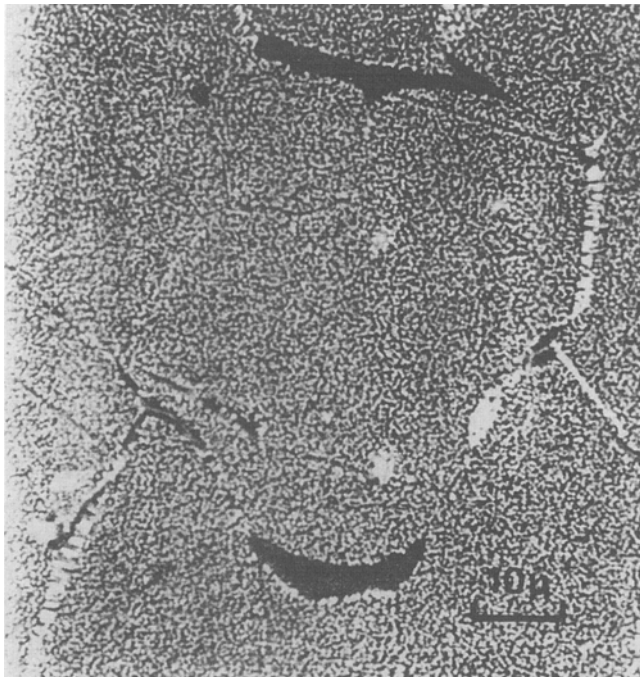
However, there are large differences in hydrostatic pressure between different regions of  $\gamma$  in an alloy which has suffered appreciable creep. For example, Pollock and Argon<sup>[5]</sup> estimated that after a creep strain of  $6 \times 10^{-3}$ , the hydrostatic pressure in the transverse channels of their sample of CMSX-3 was about -400 MPa, while that in the lateral channels was about 50 MPa, making a pressure difference of  $\Delta p = 450$  MPa. Taking the atomic volume of nickel to be  $11 \times 10^{-30} \text{ m}^3$  and that of aluminum to be  $17 \times 10^{-30} \text{ m}^3$ , the difference of atomic volumes is  $\Delta V = 6 \times 10^{-30} \text{ m}^3$ .

The change of free energy if an aluminum atom in a transverse interface exchanges with a nickel atom in a lateral interface is  $\Delta p\Delta V = 2.7 \times 10^{-21} \text{ J}$ . The experimental evidence is far from clear, but it appears from References 28 and 29 that the differences of concentration along a diffusion path are at most of order 10 pct. The change of free energy arising from this difference of concentration when one atom diffuses from a transverse channel to a lateral channel is then  $kT \ln 1.1$ . With  $k = 1.4 \times 10^{-23} \text{ JK}^{-1}$  and  $T = 1350 \text{ K}$ , this is  $1.8 \times 10^{-21} \text{ J}$ , appreciably less than the change induced by the pressure gradient. Svetlov *et al.*<sup>[28]</sup> explained their observations qualitatively in this way. On the other hand, the observations<sup>[29]</sup> on the commercial superalloy CMSX-2, which shows normal rafting, are difficult to rationalize in terms of these considerations.

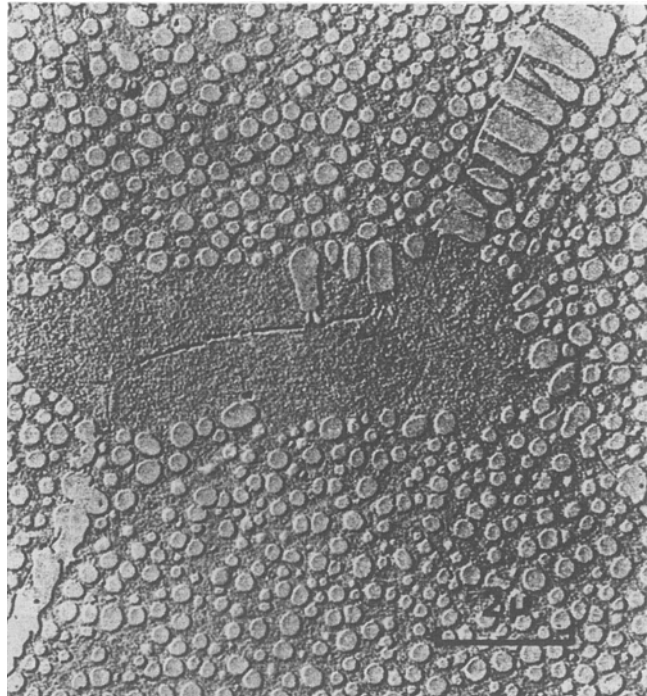
According to Eq. [5], the initial rate of rafting should be linear in the applied stress  $\sigma$ . Figure 19, taken from Reference 30, shows a rate which is roughly linear in stress at low temperatures and high stresses in the range 186 to 234 MPa but which increases much more than linearly with the stress at high temperatures and low stresses in the range 147 to 179 MPa. This suggests that there is a barrier to changes in the shape of the interface, which can be overcome by a stress of order 160 MPa. A possible mechanism for this barrier is that the  $\gamma/\gamma'$  interface is composed of  $\{100\}$  terraces, with layers alternately NiAl and Ni in  $\gamma'$   $\text{Ni}_3\text{Al}$ , and disordered in  $\gamma$ . The growth of  $\gamma'$  requires the nucleation of fresh layers of NiAl, and the rough calculation in the Appendix suggests that this nucleation will occur at an appreciable rate only under external stresses which exceed a critical value estimated at 410 MPa, of the same order as the critical stress suggested by the observations. On the other hand, one may extract data from the observations of Reference 31 which are more compatible with a simple linear law than with the existence of a threshold stress (Figure 20).

## IX. HOW DOES RAFTING INFLUENCE CREEP? THEORETICAL

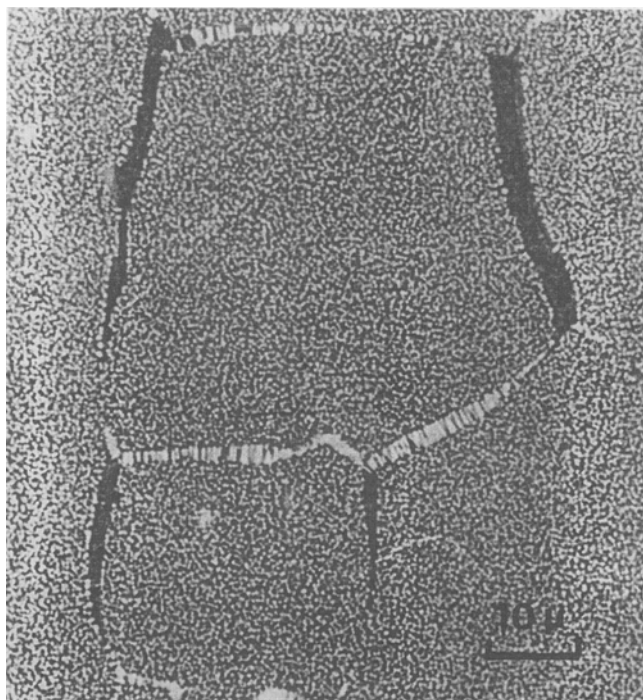
Since rafting is induced by external stress, this stress must do work while rafting occurs. That is to say, rafting is a mechanism of creep. Suppose the creep strain is  $\varepsilon_c$ . Then an external stress  $\sigma$  has done work  $w^3 a^3 \varepsilon_c \sigma$  on each  $\gamma/\gamma'$  supercell. Half of this work is stored and half dissipated,



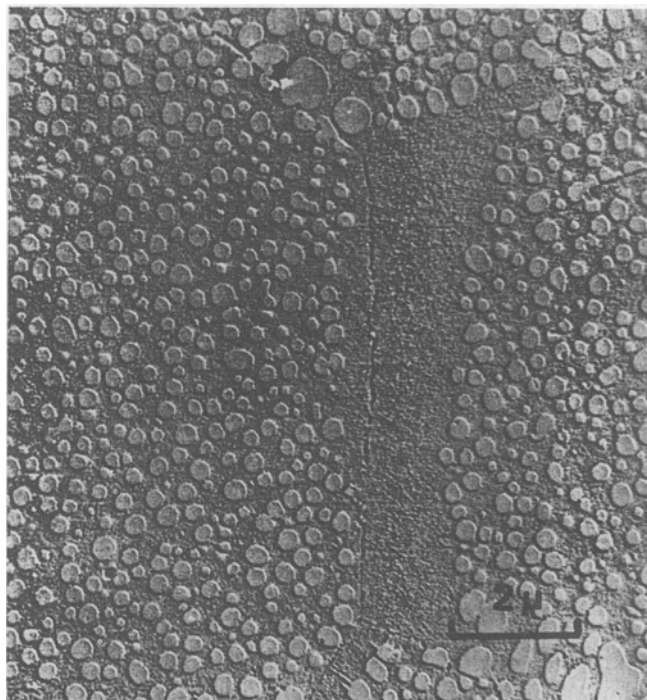
(a)



(b)



(c)



(d)

Fig. 18—Creep in an alloy probably having a very small misfit, showing diffusional creep at the grain boundaries but none at the  $\gamma/\gamma'$  interfaces, and negligible rafting: (a) and (b) under tension, markers 10  $\mu$ , 2  $\mu$ ; and (c) and (d) under compression.<sup>[27]</sup>

pated. Equating the work dissipated to that given by Eq. [5], we find

$$\varepsilon_c = \frac{4c^*(c_{11} + 2c_{12})}{c_{11}(c_{11} - c_{12})} |\delta\varepsilon| \quad [9]$$

Inserting the values  $c^* = 12$  GPa,  $c_{11} = 110$  GPa,  $c_{12} = 60$  GPa, and  $\delta = 1.4 \times 10^{-3}$  appropriate to CMSX-2, this gives

$$\varepsilon_c = 2.8 \times 10^{-3} |\varepsilon| \quad [10]$$

Adjacent cubes of  $\gamma'$  meet and fuse to form rafts at about  $\varepsilon = 0.16$ . The corresponding bulk strain is  $\varepsilon_c = 4.5 \times 10^{-4}$  and is almost negligible.

However, the resulting rafted microstructure is completely different from the original array of cubical  $\gamma'$  particles, and its behavior in later stages of creep may be quite different. The effects are expected to be different at high

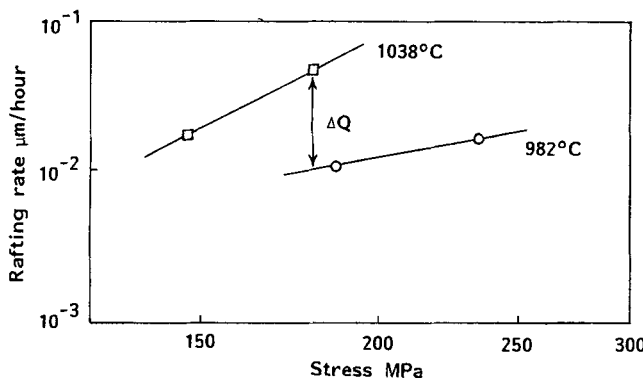


Fig. 19—Speed of  $\gamma/\gamma'$  interface as a function of temperature and stress.<sup>[30]</sup>

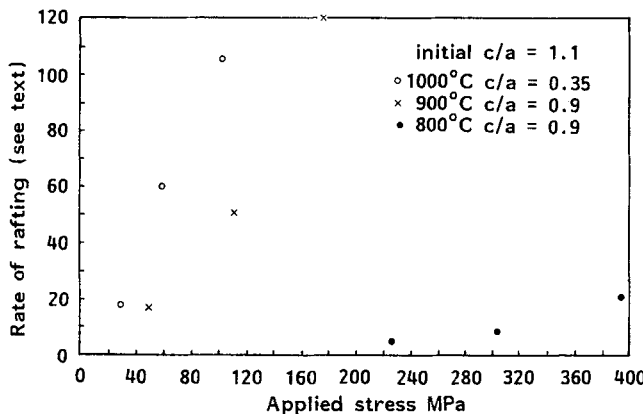


Fig. 20—Rate of rafting measured by  $1000/(\text{number of hours to obtain a prescribed axial ratio } c/a \text{ from an initial value } c/a = 1.1)$ , as a function of stress at a given temperature:  $\circ$  1000 °C,  $c/a = 0.35$ ;  $\times$  900 °C,  $c/a = 0.9$ ;  $\bullet$  800 °C,  $c/a = 0.9$  (from the data in Ref. 31).

and low temperatures. At high temperatures, dislocation climb is easy, the  $\gamma$  phase flows like a viscous liquid around the  $\gamma'$  particles, which remain rigid under the relatively low stresses which lead to an acceptable rate of creep. Rafting lengthens the channels through which the matrix must flow, or, in dislocation terms, increases the distance through which dislocations have to climb, and so<sup>[30,32-37]</sup> reduces the rate of creep. At lower temperatures, the viscosity of the  $\gamma$  phase is higher, the operating stresses are higher, and the dislocations are able to cut through the  $\gamma'$  phase. It is generally accepted that the coarser microstructure produced by rafting facilitates this process of plastic shear in  $\gamma'$ . The mechanism seems to be as follows.

The calculations of Pollock and Argon<sup>[5]</sup> showed (Figure 21) that the shear stress in the  $\gamma$  channels is remarkably uniform, being the stress required to maintain the local strain rate in a medium with a rapid dependence of strain rate on stress (Figure 20(a)). In this case, after creep has occurred for  $2.4 \times 10^5$  seconds, the shear stress is around 45 MPa. Much bigger hydrostatic stresses build up in the matrix, from -400 MPa in the transverse channels to +80 MPa in the lateral channels (Figure 21(b)). This corresponds to a shear stress of about 480 MPa in the  $\gamma'$  particles. The calculated plots of shear stress in the matrix (Figures 21(c) and (d)) are for periods of creep of  $1.1 \times 10^5$  and  $4.3 \times 10^5$  seconds, bracketing the time of  $2.4 \times 10^5$  seconds in Figures 21(a) and (b). They show remarkably uniform shear stresses in the  $\gamma'$  of 220 and 900 MPa,

respectively, bracketing the value of 500 MPa which we have estimated for  $2.4 \times 10^5$  seconds. These shear stresses ultimately allow single dislocations to pass through the  $\gamma'$ , trailing planar defects behind them. In dislocation terms, the discontinuity in the stress field at the  $\gamma/\gamma'$  interface is the stress field of the dislocations accumulated on this interface. Now suppose we carry out a similar analysis for a rafted specimen. The shear stress in the  $\gamma$  phase is still equal to the flow stress. This implies that the gradient of hydrostatic pressure along a streamline is the same as in the unrafted material. The streamlines are now longer, the difference of hydrostatic pressure between the middle of a transverse channel and a lateral channel is larger, the shear stress in  $\gamma'$  is larger, and dislocations penetrate  $\gamma'$  more readily. This effect has been directly observed in NASAIR 100 at 760 °C and stresses of 600 to 820 MPa.<sup>[38]</sup>

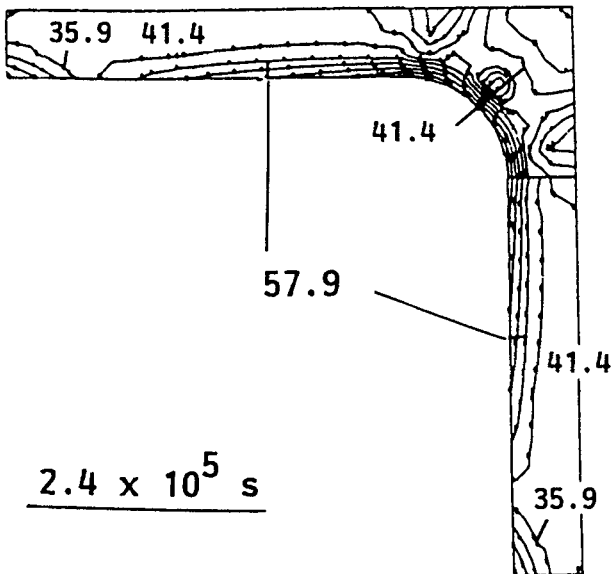
All the observations of References 30 and 32 through 37 conform to the general pattern that rafting improves the creep performance when dislocations do not penetrate the  $\gamma'$  phase and worsens it when the  $\gamma'$  particles are cut by dislocations.

Some observations on more modern alloys seemed to imply that rafting always reduced the creep resistance. Thus,<sup>[39]</sup> prerafting increased the creep rate of SRR99 at 900 °C or 1050 °C. In CMSX-4 at 800 °C and 950 °C,<sup>[40]</sup> rafting "was found to deteriorate the creep properties under the given test conditions." However, "stacking faults are seen clearly" (though not abundantly), so that this observation is compatible with the view that rafting reduces the creep resistance when dislocations penetrate the  $\gamma'$  phase. Measurements on CMSX-4 at 1100 °C<sup>[41]</sup> concluded: "Rafts do not form at 800 °C. At 950 °C raft formation always leads to an enhanced creep rate (softening), accompanied by dislocation cutting of the  $\gamma'$  rafts. At 1100 °C raft formation is accompanied by a reduced creep rate (hardening) without cutting of the  $\gamma'$  rafts. Then, the creep rate increases (softening) as  $\gamma'$  raft cutting and further coarsening occur." Hammer<sup>[42]</sup> found that CMSX-4 tested at 1050 °C under 150 MPa showed a longer creep life after prerafting. It seems fair to say that we now know the underlying mechanisms of these effects.

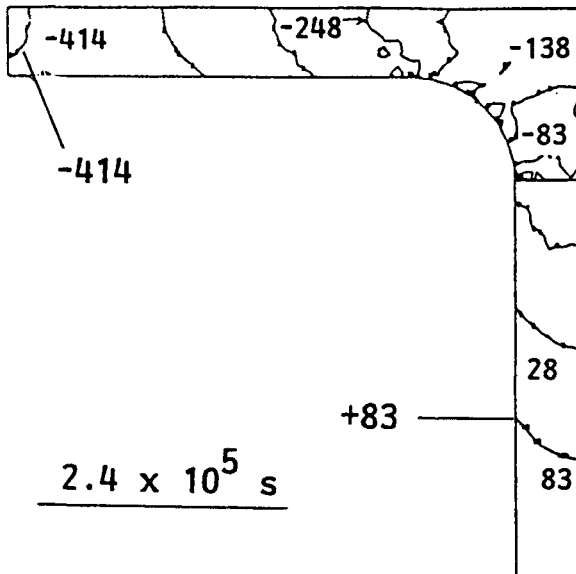
## X. ARE THERE IMPLICATIONS FOR ALLOY DESIGN?

The attitude of senior design engineers<sup>[43,44]</sup> is that rafting is a fact of life and that it is pointless to try to control it. According to the present discussions, rafting is controlled mainly by the lattice misfit  $\delta$  and to a lesser extent by the elastic mismatch  $c^*$ . The rate of rafting increases with  $|\delta|$ , but rafting occurs so early in the service life that changes in this rate are probably unimportant. It is not clear whether the critical regions in a turbine blade are in the high-temperature low-stress region where rafting suppresses creep or in the low-temperature high-stress region where rafting accelerates creep.

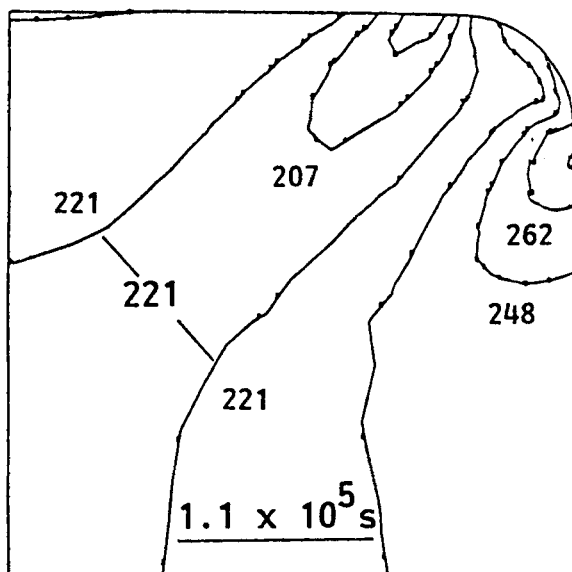
An almost consistent picture emerges from the fact that almost all modern commercial superalloys have small negative values of  $\delta$ , so that rafts form transverse to the axis of a tensile stress in the dominant Socrate-Parks regime. This does not necessarily imply that rafting is desirable, only that transverse rafts are better than longitudinal rafts



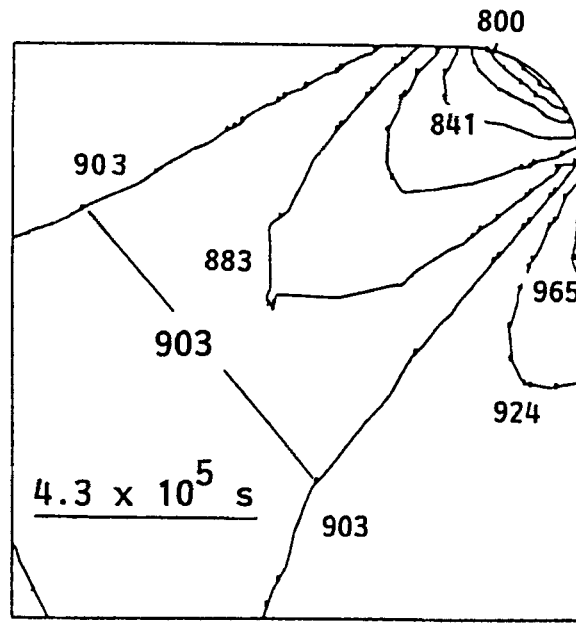
(a)



(b)



(c)



(d)

Fig. 21—Calculated stresses during creep of CMSX-3: (a) rather uniform shear stress  $\approx 45$  MPa in the matrix after  $2.4 \times 10^5$  s; (b) hydrostatic stresses in the matrix regions varying from  $-400$  to  $+80$  MPa after the same time, implying a shear stress in  $\gamma'$  of the order 480 MPa; (c) and (d) the calculated shear stresses in  $\gamma'$  after  $1.1 \times 10^5$  and  $4.3 \times 10^5$  s, bracketing the time for (a) and (b), are about 220 and 900 MPa, respectively, compatible with the estimated 480 MPa. Reprinted from Ref. 5 with the kind permission of Elsevier Science Ltd.

or needles. Since  $m$  is generally positive, the sense of rafting is the same in the early and in the later stages of creep, which means that the transverse rafts are well developed, which does seem to imply that rafting is beneficial. It may well be that the positive value of  $m$  is not a consequence of successful alloy design but an almost inevitable consequence of ordering in the  $\gamma'$  phase.

Given that the misfit  $\delta$  should be negative, why should it be small? In an alloy hardened by a dilute dispersion of coherent particles, a large misfit produces large random stresses in the matrix which hinder dislocation motion and add strength. In a modern superalloy, the misfit stresses are almost constant throughout each sheet of matrix, and this argument does not apply.

The practical use of alloys with small misfits is contrary to much experimental evidence favoring alloys with large misfits. Thus, one article<sup>[45]</sup> summarizing results on alloys with a  $\gamma'$  volume fraction of about 56 pct shows clearly (Figure 22) that alloys with high misfit have high creep resistance. Moreover, the high misfit does not appear to inhibit the development of a small particle size. An earlier article<sup>[26]</sup> quoted six studies favoring a small misfit and four favoring a large misfit. A detailed study<sup>[46]</sup> concerned a series of alloys containing 6 wt pct Al, 6 wt pct Ta, and 9.8 to 14.6 wt pct Mo. Up to about 14 pct Mo, where a third phase (the intermetallic NiMo with a complex structure) appears, the creep properties steadily increase with increasing Mo content, which is coupled with an increasing neg-

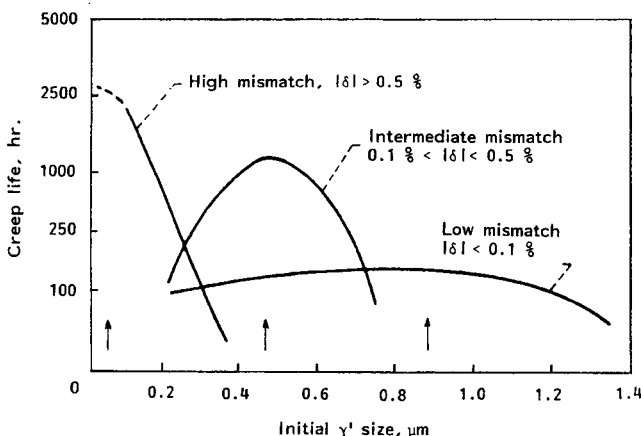


Fig. 22—Creep lives for alloys with various misfits and various initial  $\gamma'$  sizes. The alloys with large misfits have the longest creep lives.<sup>[45]</sup>

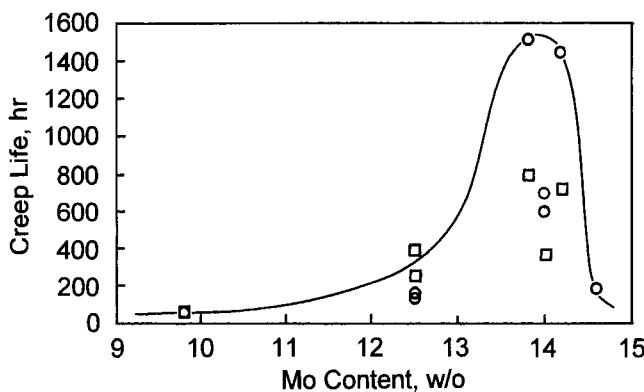


Fig. 23—Creep lives at 982 °C and 234 MPa of experimental alloys, as a function of molybdenum content.<sup>[46]</sup>

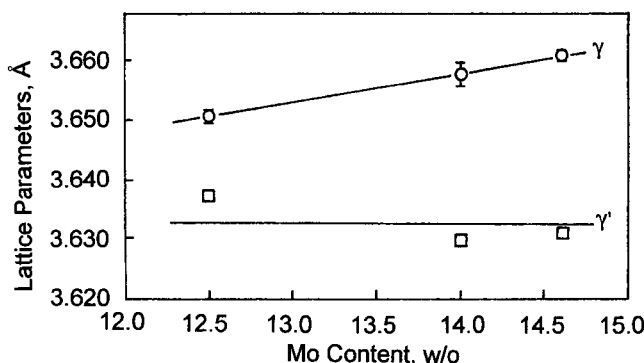


Fig. 24—Lattice parameters of  $\gamma$  and  $\gamma'$  at 982 °C in the alloys of Fig. 23.<sup>[46]</sup>

ative misfit (Figure 23). The lattice parameter of  $\gamma'$  remains constant, while that of  $\gamma$  increases (Figure 24), so the Mo must be dissolved principally in the  $\gamma$  phase. Solid-solution hardening of the  $\gamma$  may therefore make a large contribution to the creep strength, particularly because the proximity of the NiMo phase boundary and the very rapid changes in the creep properties near this boundary suggest the possibility of substantial clustering of Mo atoms in the  $\gamma$  phase. There is much evidence of strong short-range order in Ni-Mo alloys,<sup>[47,48]</sup> and it is of a kind involving tetragonal distortions and thus strong resistance to dislocation motion.

How could a large misfit adversely affect the creep properties? Perhaps the observations of Figure 23 illustrate a

more general phenomenon, that alloying elements which increase the  $\gamma'/\gamma$  misfit tend to form undesirable intermetallic compounds in the  $\gamma$  phase. There may be another argument which applies in the low-temperature high-stress regime. Consider the case of a negative-misfit alloy under tension. Creep begins over the transverse interfaces. The dislocations deposited on these interfaces readjust to form misfit dislocations, relieving the misfit stresses. Later, plastic deformation spreads to the lateral  $\gamma$  channels, depositing on the interfaces dislocations which have the wrong sign to relieve the misfit. If these  $1/2\langle 011 \rangle$  dislocations penetrate the  $\gamma'$  phase, either unchanged or, as is usual in practice, after reacting to produce  $1/2\langle 111 \rangle$  partials, they both relieve the local strain and allow the applied stress to do work. As soon as plastic flow is initiated in the  $\gamma'$  phase, the creep resistance of the whole structure is reduced. (In discussion after the meeting, A.F. Giamei suggested the following interpretation: A large misfit is generally desirable but accelerates Ostwald ripening. When the operating temperature is increased, the optimum misfit is reduced. When an element such as rhenium is introduced to decrease the rate of diffusion, the optimum misfit again increases.)

## APPENDIX The barrier to rafting

If the configurational force for rafting is linear in the applied stress, and the mechanism of rafting is controlled by diffusion, the rate of rafting should be linear in the applied stress. The experimental evidence is limited. MacKay and Ebert<sup>[30]</sup> reported results (Figure 19) for a "model superalloy" at two temperatures. At 982 °C and 186 to 234 MPa, the stress dependence is not far from linear though slightly more rapid, but at 1038 °C and 147 to 179 MPa, the rate of rafting depends very strongly on stress. If this change were produced by some mechanism involving the glide of dislocations, one would expect the strong dependence on stress to appear at high stresses, as in the progression from Nabarro-Herring creep and Harper-Dorn creep through power-law creep to power-law breakdown. A high stress dependence at low stresses suggests that these low stresses are approaching some critical frictional or nucleation stress below which rafting can occur only very slowly. This stress would be of the order of 160 MPa. We now suggest a possible origin of this stress.

Farkas *et al.*<sup>[49]</sup> studied theoretically the structure of the {100} interface between  $\gamma'$  Ni<sub>3</sub>Al and pure nickel, and we assume that similar considerations may apply to a  $\gamma'/\gamma$  interface. Alternate {200} planes in Ni<sub>3</sub>Al are filled with all nickel atoms and with equal numbers of nickel and aluminum atoms. The {100}  $\gamma'/\text{Ni}$  interface has its lowest energy when the nickel {200} planes adjoin all-nickel {200} planes in Ni<sub>3</sub>Al. Migration of this interface requires the nucleation of an interface between a NiAl {200} plane and a {200} plane in nickel. The interfacial energies  $\Gamma$  are of order 20 mJ m<sup>-2</sup>. At 1000 K, the thermal energy  $kT$  is of order  $1.4 \times 10^{-20}$  J.

We picture the interface as consisting of terraces of Ni/Ni interfaces separated by cliffs of height one superlattice cube edge  $a$ , about  $5 \times 10^{-10}$  m. The energy of such a ledge will be of order  $\Gamma a \approx 10^{-11}$  J m<sup>-1</sup>. A new terrace is likely to nucleate from a corner of a cube face in the form of a

quadrant of radius  $r$ . It requires little energy to form the straight edges of this quadrant, which lie along rounded edges of the cube, but the curved edge has energy  $\frac{1}{2} \pi r^2 \Gamma a$ . If the configurational pressure tending to produce rafting is  $p_c$ , this pressure does work  $\frac{1}{4} \pi r^2 p_c a$  when the quadrant is formed.

The increase in enthalpy is thus

$$\Delta H = \frac{1}{2} \pi r^2 \Gamma a - \frac{1}{4} \pi r^2 p_c a \quad [\text{A1}]$$

This has a maximum as a function of  $r$  when

$$r = \Gamma / p_c \quad [\text{A2}]$$

and the maximum is

$$\Delta H_m = \pi \Gamma^2 a / 4 p_c \quad [\text{A3}]$$

This maximum  $\Delta H_m$  is the activation enthalpy for the process, and we assume that the process will occur at an observable rate when

$$\Delta H_m \approx 30 \text{ kT} \quad [\text{A4}]$$

or

$$p_c = \pi \Gamma^2 a / 120 \text{ kT} \quad [\text{A5}]$$

While the entropies of the ground state and of the activated state may differ, we assume that this difference will be almost independent of stress and will not affect the slopes of the lines in Figure 19.

With the values  $\Gamma = 20 \text{ mJ m}^{-2}$ ,  $a = 5 \times 10^{-10} \text{ m}$ ,  $k = 1.4 \times 10^{-23} \text{ J K}^{-1}$ , and  $T = 1280 \text{ K}$ , the estimated critical configurational pressure is

$$p_c = 0.29 \text{ MPa} \quad [\text{A6}]$$

The radius of the critical quadrant is  $r = \Gamma / p_c = 7 \times 10^{-7} \text{ m}$ .

According to Eqs. [7] and [8] in the main text, rafting is driven by a difference in configurational pressures on the transverse and lateral interfaces of

$$p_c = c^* (c_{11} + 2c_{12}) \delta \sigma / c_{11} (c_{11} - c_{12}) \quad [\text{A7}]$$

where  $\sigma$  is the externally applied stress and  $\delta$  is the misfit.

With the typical values for CMSX-2 of  $c^* = 12 \text{ GPa}$ ,  $c_{11} = 110 \text{ GPa}$  and  $c_{12} = 60 \text{ GPa}$ , this becomes

$$p_c = 0.5 \delta \sigma \quad [\text{A8}]$$

Equating this configurational pressure to the critical configurational pressure given by Eq. [A6] gives

$$\sigma = (0.29 / 0.5) \delta \text{ MPa}$$

or, with  $\delta = 1.4 \times 10^{-3}$ ,

$$\sigma = 410 \text{ MPa} \quad [\text{A9}]$$

which is of the same order of magnitude as the stress of 160 MPa suggested by the observations.

On the other hand, one may analyze the data of Ohe and Wakita<sup>[31]</sup> and arrive at the conclusion that there is no critical stress for rafting. Their  $\gamma'$  particles had an initial axial ratio of  $c/a = 1.1$ , and we define the rate of rafting at a given temperature to be  $1000 / (\text{number of hours to reach a prescribed axial ratio})$ . For tests at  $1000^\circ\text{C}$ , this prescribed ratio is  $c/a = 0.35$ , and  $900^\circ\text{C}$  and  $800^\circ\text{C}$ ,  $c/a = 0.9$ . The

results (Figure 20) are compatible with a rate linear in stress at  $1000^\circ\text{C}$  and not deviating significantly from linearity at  $900^\circ\text{C}$ .

## REFERENCES

1. T. Khan, P. Caron, and C. Duret: in *Superalloys 1984*, M. Gell, C.S. Kortovich, R.H. Bricknell, W.B. Kent and J.F. Radovich, eds., TMS-AIME, Warrendale, PA, 1984, p. 145.
2. J.K. Tien and R.P. Gamble: *Metall. Trans.*, 1972, vol. 3, pp. 2157-62.
3. S. Spangenberg, H. Biermann, and H. Mughrabi: University of Erlangen-Nürnberg, unpublished work, 1994.
4. T. Miyazaki, K. Nakamura, and H. Mori: *J. Mater. Sci.*, 1979, vol. 14, p. 1827.
5. T.M. Pollock and A.S. Argon: *Acta Metall. Mater.*, 1992, vol. 40, p. 1.
6. Y. Kondo, N. Kitazaki, J. Namekata, N. Ohi, and H. Hattori: *Tetsuto-Hagané (Iron and Steel)*, 1994, vol. 80, p. 76.
7. A. Fredholm and J.L. Strudel: in *Superalloys 1984*, M. Gell, C.S. Kortovich, R.H. Bricknell, W.B. Kent and J.F. Radovich, eds., TMS-AIME, Warrendale, PA, p. 211.
8. V. Sass: Ph.D. Thesis, Universität Erlangen-Nürnberg, Nürnberg, Germany, 1993.
9. W.S. Walston and R. Darolia: GE Aircraft Engines, Cincinnati, private communication, 1994.
10. A.G. Khachaturyan: *Theory of Structural Transformations in Solids*, John Wiley, New York, NY, 1983, p. 216.
11. M.V. Nathal, R.A. MacKay, and R.G. Garlick: *Scripta Metall.*, 1988, vol. 22, p. 1421.
12. A. Pineau: *Acta Metall.*, 1976, vol. 24, p. 559.
13. G. Colonnetti: *Atti Accad. Naz. Lincei R.*, 1915, vol. 24 (1), p. 404.
14. F.R.N. Nabarro, C.M. Cress, and P. Kotschy: *Acta Metall. Mater.*, 1995, in press.
15. J.D. Eshelby: *Proc. R. Soc. A*, 1952, vol. 241, p. 376.
16. J.D. Eshelby: *Progr. Solid Mech.*, 1961, vol. 2, p. 87.
17. S. Socrate and D.M. Parks: *Acta Metall. Mater.*, 1993, vol. 41, p. 2185.
18. R.D. Field, T.M. Pollock, and W.H. Murphy: in *Superalloys 1992*, S.D. Antolovich, R.W. Sturz, R.A. MacKay, D.L. Anton, T. Khan, R.D. Kissinger and D.L. Klarstrom, eds., TMS, Warrendale, PA, p. 557.
19. J.Y. Buffière and M. Ignat: *Acta Metall. Mater.*, 1995, vol. 43, p. 1791.
20. T.M. Pollock and A.S. Argon: *Acta Metall. Mater.*, 1994, vol. 42, p. 1859.
21. H. Yasuda, T. Takasugi, and M. Koiwa: *Acta Metall. Mater.*, 1992, vol. 40, p. 281.
22. J.F. Ganghofer, A. Hazotte, S. Denis, and A. Simon: *Scripta Metall. Mater.*, 1991, vol. 25, p. 2491.
23. L. Müller, V. Glatzel, and M. Feller-Kniepmeier: *Acta Metall. Mater.*, 1992, vol. 40, p. 1321.
24. D. Ayrault, A. Fredholm, and J.L. Strudel: in *Advanced Materials and Processing Techniques for Structural Applications*, T. Khan and A. Lasalmonie, eds., Office National d'Etudes et de Recherches Aerospatiales, Chatillon Cedex, France, 1987, p. 71.
25. D.A. Grose and G.S. Ansell: *Metall. Trans. A*, 1981, vol. 12A, pp. 1631-45.
26. M.V. Nathal, R.A. MacKay, and R.G. Garlick: *Mater. Sci. Eng.*, 1985, vol. 75, p. 195.
27. J.K. Tien and R.P. Gamble: *Metall. Trans. A*, 1971, vol. 2, pp. 1663-67.
28. I.I. Svetlov, B.A. Golovko, A.I. Epishin, and N.P. Abalakin: *Scripta Metall. Mater.*, 1992, vol. 26, p. 1353.
29. J. Buffière, M.-C. Cheynet, and M. Ignat, LTPCM/ENSGEG, St. Martin d'Hères, France, unpublished research, 1994.
30. R.A. MacKay and L. Ebert: *Metall. Trans. A*, 1985, vol. 16A, pp. 1969-82.
31. J. Ohe and S. Wakita: in *Superalloys 1984*, M. Gell, C.S. Kortovich, R.H. Bricknell, W.B. Kent and J.F. Radovich, eds., TMS-AIME, Warrendale, PA, 1984, p. 93.
32. D.D. Pearson, F.D. Lemkey, and B.H. Kear: in *Superalloys 1980*, J.K. Tien, S.T. Wiodek, H. Morrow III, M. Gell and G.E. Maurer, eds., ASM, Metals Park, OH, 1980, p. 513.

33. D.D. Pearson, B.H. Kear, and F.D. Lemkey: in *Creep and Fracture 1981*, B. Wilshire and D.R.J. Owen, eds., Pineridge Press, Swansea, 1981, p. 213.
34. P. Caron and T. Khan: *Mater. Sci. Eng.*, 1983, vol. 61, p. 173.
35. M.V. Nathal and L.J. Ebert: *Metall. Trans. A*, 1985, vol. 16A, pp. 427-39.
36. M.V. Nathal and L.J. Ebert: *Metall. Trans. A*, 1985, vol. 16A, pp. 1863-70.
37. P. Caron, P.J. Henderson, T. Khan, and M. McLean: *Scripta Metall.*, 1986, vol. 20, p. 875.
38. M.V. Nathal, R.A. MacKay, and R.V. Miner: *Metall. Trans. A*, 1989, vol. 20A, pp. 133-41.
39. J. Hammer and H. Mughrabi: *Proc. 1st Eur. Conf. on Advanced Materials and Processes, EUROMAT '89*, D. Driver and H. Mughrabi, eds., Informationsgesellschaft-Verlag, D-6370 Oberursel, Germany, 1989, vol. 1, p. 445.
40. W. Schneider, J. Hammer, and H. Mughrabi: in *Superalloys 1992*, S.D. Antolovich *et al.*, eds., TMS, Warrendale, PA, 1992, p. 589.
41. H. Mughrabi, W. Schneider, V. Sass, and C. Lang: *Proc. 10th Int. Conf. Strength of Metals and Alloys, ICSMA 10*, H. Oikawa, K. Maruyama, S. Takeuchi and M. Yamaguchi, eds., Japan Institute of Metals, Sendai, Japan.
42. J. Hammer: Ph.D. Thesis, University Erlangen-Nürnberg, Nürnberg, Germany, 1990.
43. Anon: private communication, 1994.
44. Anon: private communication, 1994.
45. M.V. Nathal: *Metall. Trans. A*, 1987, vol. 18A, pp. 1961-70.
46. R.A. MacKay, M.V. Nathal, and D.D. Pearson: *Metall. Trans. A*, 1990, vol. 21A, pp. 381-88.
47. K.H. Lee, K. Hirago, D. Shindo, and M. Hirabayashi: *Acta Metall.*, 1988, vol. 36, p. 641.
48. M. Yamamoto, Y. Takeshita, J. Tada, and K. Nishikana: *Appl. Surf. Sci.*, 1994, vol. 76-77 (76), p. 184.
49. P. Farkas, M.F. de Campos, R.M. de Souza, and H. Goldenstein: *Scripta Metall. Mater.*, 1994, vol. 30, p. 367.